WIRELESS POWER TRANSFER:

A RECONFIGURABLE PHASED ARRAY WITH NOVEL FEEDING ARCHITECTURE

A Thesis

Submitted to the Faculty

of

Purdue University

by

Mitchel H Szazynski

In Partial Fulfillment of the

Requirements for the Degree

of

Master of Science in Electrical and Computer Engineering

May 2018

Purdue University

Indianapolis, Indiana

TABLE OF CONTENTS

Page

LIST OF FIGURES

Figure Page

Figure Page

ABSTRACT

Szazynski, Mitchel H. M.S.E.C.E., Purdue University, May 2018. Wireless Power Transfer: A Reconfigurable Phased Array with Novel Feeding Architecture. Major Professor: Peter J. Schubert.

This thesis proposes a reconfigurable phased array of antennas for wireless power transfer. The array finds use in many applications, from drone destruction (for defense) to wireless charging of robots and mobile devices. It utilizes a novel feeding architecture to greatly reduce the number of high cost elements (such as amplifiers and phase shifters) as well as the quantity of unused resources in the system.

Upon the instruction of the CPU, the array can separate into any number of subarrays, each of which transmits power to a single receiver, steering its beam as the receiver changes location. Currently dormant elements in the array can be used to provide position information about the receivers, either via Radar, or by listening for beacons pulses from the receiver.

All of this is made possible, with only 4 amplifiers and 3 phase shifters, by the proposed 4-Bus Method. The source signal is divided into four buses, which are respectively phase shifted by 270 degrees, 180 degrees, 90 degrees, and 0 degrees (no shifter required) and then amplified. The CPU calculates, based on the number and positions of the receivers / targets, what the amplitude and phase excitation must be at each element. Any phase and amplitude which could be required can be achieved by simply adding together appropriate quantities of the correct two buses. In order to achieve this, the key piece is the variable power divider. These differ from Wilkinson dividers in that the dividing ratio can be changed via an applied DC voltage. Therefore, at each junction, by properly diverting the power levels on each phase bus to their proper location, complete delocalization of both amplifiers and phase shifters can be achieved.

A method has also been developed which helps overcome the limitations of each variable power divider. That is, in certain instances, it may be desirable to pass all the power to a single output port or the other, which is not a possibility inherently possible with the device. With the use of a unique combination of RF switches, the nodes achieve much enhanced flexibility.

Finally, an intensive study is carried out, in an attempt to yield greater understanding, as well as quick, useful approximations, of the behaviors of both rectangular and hexagonal arrays of various sizes and beam steering angles for wireless power.

1. INTRODUCTION

Wireless power transfer is a rapidly expanding field, with consumer demand as well as brand new applications driving large amounts of research dollars to be spent improving the technology. Primarily, the efforts are focused on inductive and magnetic resonant charging, for relatively short range, high efficiency power transfer, for cell phones, watches, mobile robots, and electric cars.

Some applications, however, require long range (several meters to hundreds of miles) power transmission. These include drone defense, "Space Solar Power", and more flexible systems for charging mobile receivers. The best option for these is radiative power transfer, with microwaves or millimeter waves. This is accomplished with large groups of antennas known as phased arrays, which if designed and operated properly, can not only "direct" the majority of their transmitted power toward a single desired target, but can even "steer" the direction of transmission without ever physically changing position. These phased arrays have become a vital tool in many industries today, but the exorbitant quantities of expensive devices required within the systems which operate them make their use unaffordable in some everyday applications.

This thesis explores some of the many applications of microwave and millimeter wave wireless power transfer, proposes and examines in depth a novel reconfigurable phased array for wireless power, demonstrates the merit of a one-of-a-kind array feeding architecture which dramatically reduces the number of high cost elements, and investigates the behavior of various array architectures as their size and beam steering angle is altered.

The organization of this thesis is as follows. Chapter 2 gives an introduction to many of the technical details of antenna engineering for the technically minded but unexperienced reader. Chapter 3 discusses prior work in both wireless power and phased arrays. Chapter 4 introduces the author's contribution of a reconfigurable phased array with novel feeding architecture and gives results which compare it to previously existing methods. Chapter 5

gives results on thorough studies of array behavior for various geometries, steering angles, and element spacings, with an emphasis on wireless power applications. Summary and future work are discussed in Chapter 6.

2. BACKGROUND

2.1 Antennas

An antenna is a device that converts electromagnetic waves in the air into electricity in a circuit, or visa-versa. They are useful in wireless communications (transmission of information) in such applications as telephones, television, radios, and computers. An emerging (and less known) application is that of wireless power transfer. For an antenna to radiate, it must be excited with AC power at an appropriate frequency. With traditional methodologies, this frequency should be such that the antennas physical size is approximately equal to the operating wavelength (speed of light divided by frequency).

Some common types of antennas include dipoles, microstrip (patches), slotted waveguides, parabolic dishes, and horns. Some (such as dipoles) radiate power almost equally in every direction, or are "omnidirectional". Others, such as the last three listed here, send power almost exclusively in a single direction. The microstrip has performance which is somewhat of a compromise between the two extremities.

It is certainly worthwhile to discuss some of the key figures of measuring antenna performance, in order to discuss with great brevity later in the thesis, and still be understood by as large an audience as possible.

Sterradians

In order to understand what will follow, it is necessary to have a grasp on the concept of a solid angle, measured by the "sterradian". Just as a radian is a measure pertaining to fractions of a circle, a sterradian pertains to fractions of a sphere. That is, pi radians

measure an arc of half of a circle (there are two pi radians in a circle). Because the surface area of a sphere is 4 pi times the square of the radius, there are 4 pi sterradians in a sphere of radius r. Each sterradian traces out an area of r squared at the edge of the sphere.

Radiation Intensity

Radiation intensity is exactly what it sounds like: It measures how intense the beam from the antenna is at any given angle. Mathematically, the average radiation intensity is:

$$U_0 = PowerRadiated/(4 * \pi) \tag{2.1}$$

Directivity

When considering the total power radiated by an antenna, the directivity is a measure which describes what portion of the power is transmitted in given direction. An antenna with a high directivity sends a large portion of its power to a single place. This is expressed by:

$$D_{max} = U_{max}/U_0 \tag{2.2}$$

Or alternatively, this could be shown as:

$$D_{max} = 4 * \pi * U_{max}/PowerRadiated \tag{2.3}$$

An “omnidirectional” radiator has a “radiation pattern” such as this:

In general, gain, directivity, and many other important figures of merit will be discussed in terms of decibels (dB) throughout this work. Directional antennas send (or receive) more power in one direction than another. Directivity and gain are measurements of a device’s performance in this area. By way of analogy, think of someone swinging a running hose around their head in a circle (omnidirectional). If someone else stands 10 feet away with

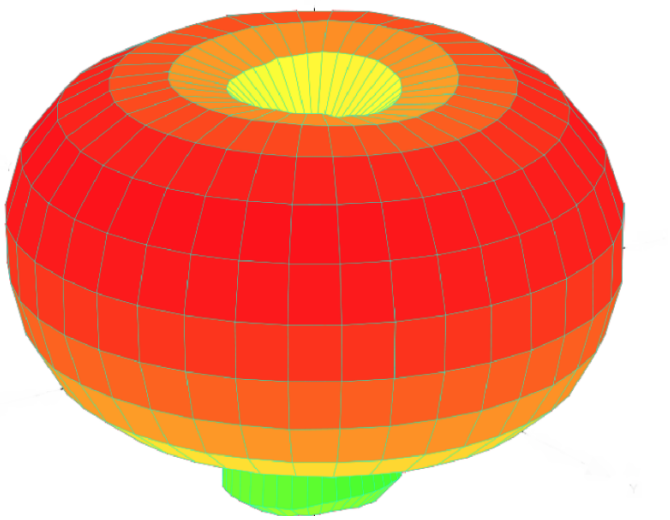

Fig. 2.1. Radiation pattern of an omnidirectional antenna [21]

a bucket, some water will doubtless land in it. However, if they turned the hose setting to "jet" and pointed it toward the bucket, the majority of the water would end up in the bucket! This is the concept of using a highly "directive" antenna.

Power Density

Measured in Watts per square meter, the power density is one of the most important measures related to electromagnetics. Average power density is:

$$Pd_{average} = PowerRadiated/(4 * \pi * r^2) \tag{2.4}$$

Where r is, as usual, the distance from the antenna. This can also be expressed as:

$$Pd_{average} = U_0/r^2 \tag{2.5}$$

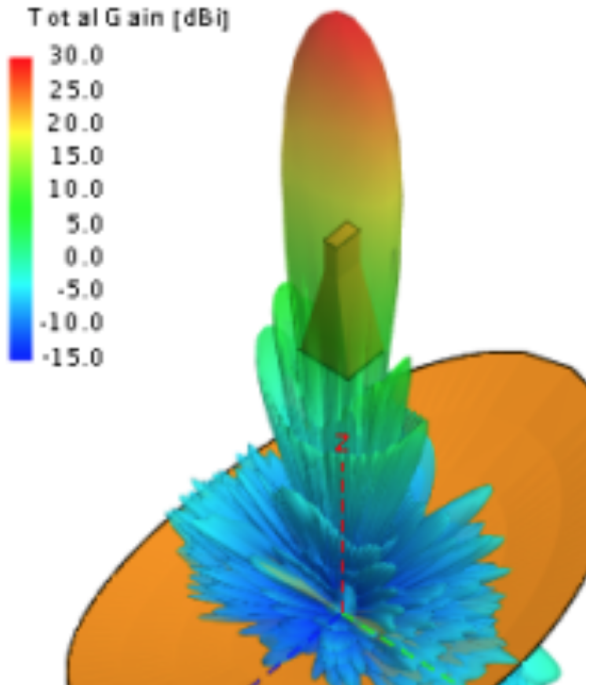

Fig. 2.2. Radiation pattern of a high directivity antenna [22]

Gain

Perhaps the single most important property of an antenna for the topics being discussed in this thesis, the gain is almost identical to the directivity, but also takes into account the internal losses of the antenna.

$$Gain = \epsilon * Directivity \tag{2.6}$$

Where epsilon takes into account all internal losses due to mismatches, internal resistances, etc.

Sidelobe Level

In a directional antenna or array, there is a “main lobe” in which the power is primarily sent. It is impossible for 100 percent of the power to be “focused”, however. The power which goes in other directions forms “sidelobes”, which are typically measured based on how many decibels lower than the main lobe they are in magnitude.

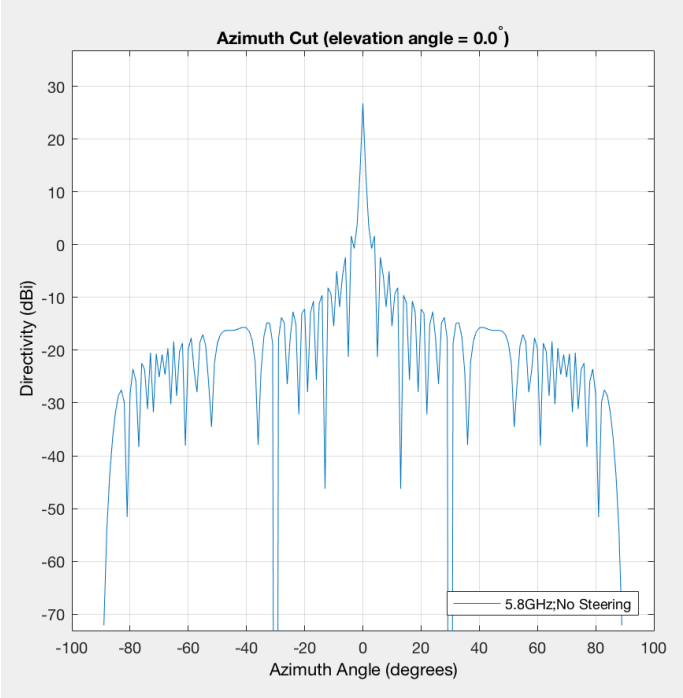

Fig. 2.3. Example of a 2-dimensional cross section of a radiation pattern

In the figure above, the largest sidelobes, with a directivity of about 2 dBi, are about 25 dB lower than the main lobe. Therefore we could say that the array has directivity of 27 dBi with -25 dB maximum sidelobe level (SLL).

Beamwidth

It is also important to know not just the magnitude of a given "lobe", but also how wide it is. This is measured in terms of sterradians (since it is a 3D, or solid angle). The most common form is the 3dB, or "half power" point beamwidth. When this is used, the measured beamwidth considers the beam to extend from maximum point until it reaches half its magnitude in each direction.

2.2 Phased Arrays

Beam Steering

Phased arrays possess superior performance in many ways over any single antenna element, even very directive ones such as parabolic dishes [2]. An additional benefit of arrays stems from the ability to steer [3]. Without arrays, an antenna must be physically turned in order to change the direction of its beam. This means bulky mechanical parts which break easily. However, by applying appropriate phase shifts between the excitations of the various array elements, the beam can be steered without ever turning the device. This is called an "electrically steerable array", or "phased array". Although it is a difficult concept to grasp, the direction of an array's beam can be changed by applying a phase shift between each antenna. Many arrays operate naturally in the "broadside mode". This means that their standard beam eminates straight out from the device, normal to its surface.

Balanis [12] describes the standard method for determining phase excitation in a linear array to be:

$$\beta = -k * d * cos(\theta) \tag{2.7}$$

Alternatively, [28] alters the terms to assume an angle of 0 is broadside, and puts it terms of degrees:

$$\phi = 360 * d * sin(\theta)/\lambda \tag{2.8}$$

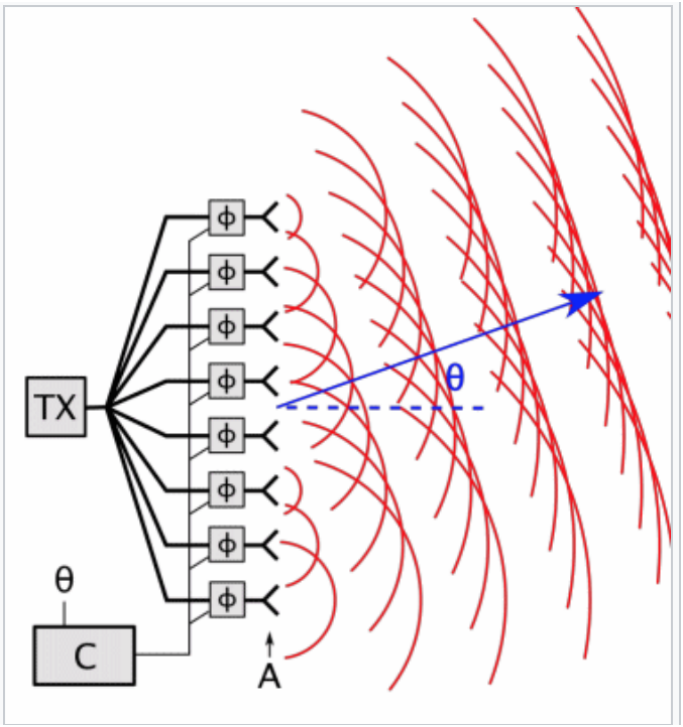

Fig. 2.4. Depiction of how phase delay can allow beam steering [20]

Where beta and phi are (equivalent) the phase shift between each element, k is the wavenumber, d is the distance between array elements, and theta is the angle at which the beam is to be steered. In the case of broadside radiation, this becomes:

$$\beta = -k * d * cos(90) = 0 \tag{2.9}$$

In other words, no phase shift is required in order to achieve broadside radiation. What if end fire radiation is desired?

$$\beta = -k * d * cos(0) = -k * d = -2 * \pi * d/\lambda \tag{2.10}$$

Obviously, this is a more complicated calculation! It should also be obvious that since this is the progressive phase shift per element, the total phase shift for any given element will be:

$$\beta_n = -n * k * d * cos(\theta) \tag{2.11}$$

Where n is the element's index in the array, or the number of steps that it is away from the first element.

For a multi-dimensional array this becomes still more involved, as you must account for two unique beam steering angles: One to determine how much the shift will be in the x direction, and another to determine the y direction. These are known as the "azmuthal" and "elevation" directions. The shift which must be applied to each element is the sum of the two, so the equation becomes:

$$\beta_n = -n * k * d * (cos(\theta_a) + cos(\theta_e)) \tag{2.12}$$

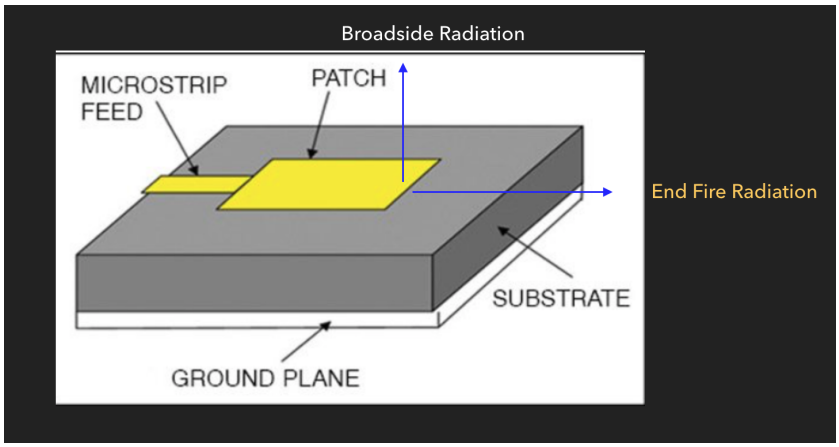

Fig. 2.5. Illustration of Broadside vs. Endfire Radiation [54]

Amplitude Tapering

An additional measurement of an antenna is its beamwidth (word of caution, this is different than its bandwidth). In general, a smaller beamwidth means that the transmitter is more precise in where it can direct its radiation (it can hit a smaller target). Therefore, having a small beamwidth is another important feature for an array to possess in order to achieve high efficiency wireless power transfer.

Amplitude tapering is the practice of exciting the elements of an array with unequal amplitudes. There are various methods for determining how to do so, but Dolph-Chebyshev Tapering guarantees the smallest possible beamwidth for a given sidelobe level. Therefore the majority of this work will use this method, in order to maximize efficiency.

Grating Lobes

Grating lobes are unintentional beams of radiation which go in the wrong direction from the main beam, and can be equal in magnitude to the main beam [11].

2.3 Wireless Power Transfer

Millions of research dollars have been spent exploring the incredible concept of transmitting power without wires. Some use magnetic induction, others use magnetically resonant coils. Some use light, and still others, microwaves. This section will discuss the existing technologies in this field.

Nikola Tesla's Wireless Power

Beginning in the 1890s, Nikola Tesla began experimenting with the transmission of electromagnetic energy with no wires. One of his proposals, the use of resonant LC circuits for wireless transmission with somewhat increased distance, is still widely used today.

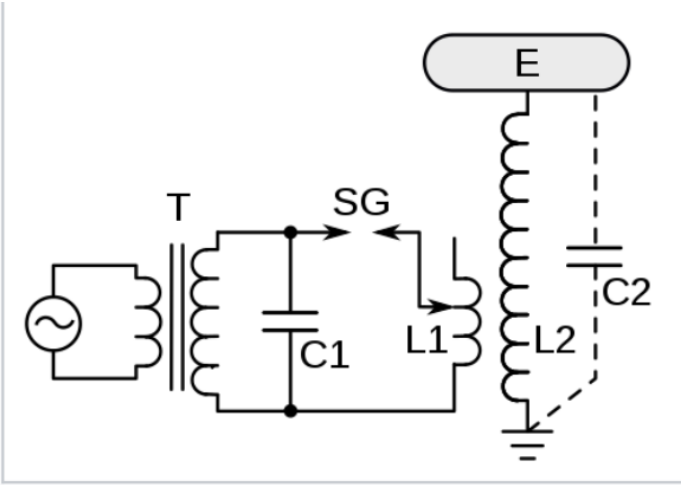

Fig. 2.6. A unipolar Tesla Coil circuit designed by Tesla for WPT [17]

One of Tesla's boldest proposals ever was his plan to transmit power around the world with his "Tesla coil", and using the earth itself as the "return path conductor". He ran extensive tests in his Colorado Springs laboratory and began construction of a tower in Shoreham, New York, shortly after the turn of the century, but his funding dried up and the project was never completed.

Inductive Wireless Power

Inductive wireless power uses essentially the technology of a transformer. By exciting one coil with an AC voltage, a voltage is induced in a nearby secondary coil, even if there is no physical connection between them. This technology is used in charging pads for mobile phones, electric toothbrushes, and mobile robots and electric cars.

This inductive technology can achieve efficiencies upward of 90 percent, but can only be operated effectively within tiny distances, less than the diameter of the coils being used.

Fig. 2.7. Example of a potential inductive WPT solution for cars [18]

Resonant Inductive Coupling

Based on proposals originally made my Nikola Tesla, Marin Soljacic led a team at MIT to develop a mid-range WPT solution in 2007. By ensuring that the transmitting and receiving coils both "resonate" at the same frequency (the frequency of operation), power can effectively be coupled between them at longer distances. Much of the "trick" in achieving this resonance is in carefully selecting values for the tuning capacitors attached at either end. Soljacic and his team ran experiments using the pictured system at 10 MHz, and were able to transmit 60 Watts of power over a distance of 8 times the coil diameter with 40 percent efficiency. Soljai then began the startup "WiTricity" based on this work [15].

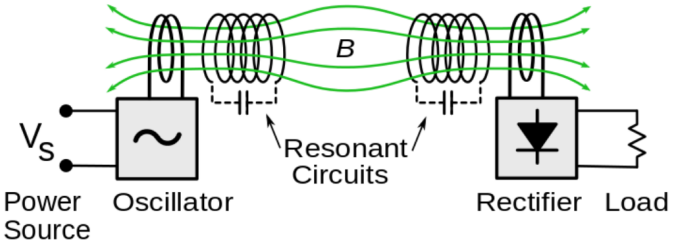

Fig. 2.8. Block diagram of a resonant inductive coupling system [15]

Lasers and Light

In terms of "directivity", it's hard to beat a laser. By its very nature, it sends out power in a very narrow beam. This aspect of it is ideal for wireless power transfer. It can be seamlessly rotated to provide power to a distant target, with minimal decrease in efficiency as the target distance increases. "LaserMotive", now known as "PowerLight Technologies", is a Seattle-based company which won the 2009 NASA Space Elevator competition. They used lasers and special photovoltaic receivers developed by Boeing to "power a small climber up a vertical tether" [4].

Aside from any safety issues to be considered, there are some disadvantages to laser power beaming. Because "light antennas", antennas small enough to operate in the visible spectrum, are not yet well developed, the only receiver for a laser is a photovoltaic "solar" cell designed to receive the appropriate frequency spectrum. These are limited to about 30-55 percent efficiency. On the transmitting end, most lasers are only about 50 percent efficiency, although a highly specialized one might reach 85 percent. Therefore, the power transfer efficiency of even the best system is current limited to between 15 and 45 percent.

Fig. 2.9. Lasers of Several different operating wavelengths [5]

Recently, “LaserMotive” changed their brand to “PowerLight Technologies” and has been doing work with “power over fiber”. This is a worthy cause in that fiber optics can be used with lower loss than standard power lines over long distances. However, it can hardly be considered “wireless”, and is still limited by the efficiency of the PV receiver.

Far-Field Microwave Wireless Power

The main topic of interest in this thesis is microwave wireless power. The benefits of this technology are clear: Long range power transmission with a highly directive steerable beam. In general, an important figure of measure for MW WPT is DC-DC conversion efficiency: That is, via the diagram pictured, DC power is used to supply AC power to a transmitting antenna or array. This power radiates across free space, and is captured by a receiving antenna or array. A rectifier is attached to this array to convert the power back into DC, and thus, the entire receiving structure is often called simply a “rectenna” [43]-[50].

William C. Brown, often known as the “Father of Microwave Wireless Power”, successfully set world records in efficiency: “92 percent RF-DC efficiency, DC-RF-DC efficiency of 54 percent at 1 KW, and later 34 kW transferred one mile with a collection efficiency of 82.5 percent”[6].

Because a high directivity antenna is essential for high efficiency, the transmitter is generally composed of either a large parabolic dish or a large array of some other type of element. Concerns for making this technology commercially available include safety issues (microwaves tend to be dangerous, obviously), but more than anything, the enormous cost of microwave components and systems is prohibitive.

3. RELATED PRIOR WORK

3.1 Phased Array Feeding Architectures

Random Phase Grouping Arrays

One proposed method for decreasing the cost of phased arrays is to replace K phase shifters by a single shifter. The shifter would service a "subarray" of the overall system, containing K antennas [23]. The result of this is some amount of phase error, arising from the loss of the resolution which was available when each element had its own shifter. The figure below illustrates both this "staircase effect" and the architecture of the system.

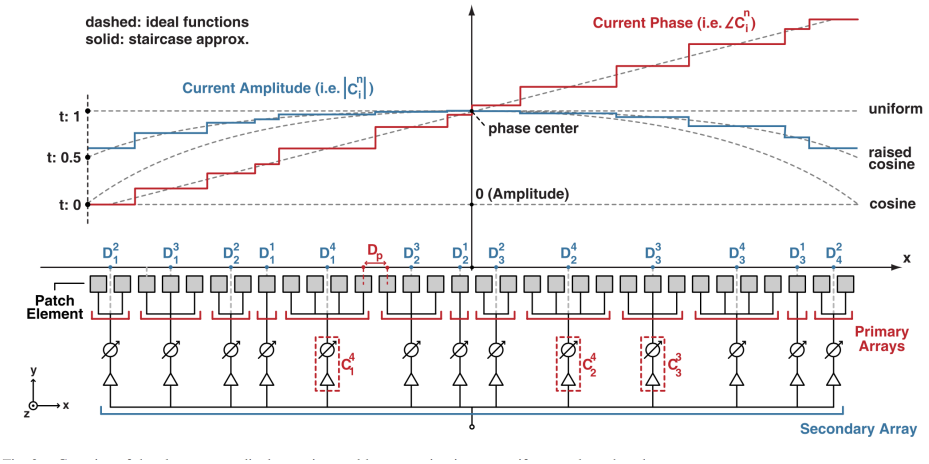

Fig. 3.1. "Staircase" Phase Error [23]

To quantify the issue at hand, phased array theory states that each successive element should receive a phase shift of:

$$\beta = -k * d * cos(\theta) \tag{3.1}$$

Where theta is the desired beam steering angle, k is the wavenumber, and d is the distance between elements. When K antennas all possess the same phase, then the edge elements will posses phase error of:

$$Error = (K-1) * \beta/2 \tag{3.2}$$

This "staircase" behavior is not dissimilar from when digital phase shifters are used, as is discussed from different perspectives in [25],[36]. In summary, this method is a simple way to reduce the number of phase shifters while creating an easily quantifiable phase error. Unfortunately, beam steering at a large angle becomes much more difficult when this technique is used, and although interesting, it is really only an option for low power applications.

Extended Resonance Technique

The extended resonance technique is a good method for "equally dividing and combining power from many devices" [24]. Using this method in phased arrays can allow the combination phase shifters and power dividers into a single circuit. An example of this technology is shown below.

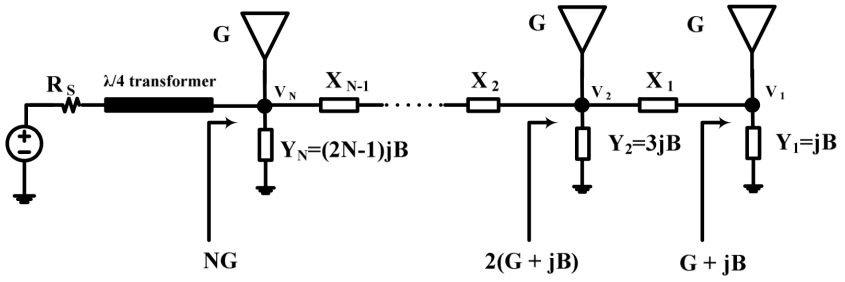

Fig. 3.2. One example of an extended resonance system [24]

The operating principle is that a varactor diode (tunable capacitor) is placed in shunt in various places along the power dividing transmission lines. By tuning the reactance, a phase shift can be achieved. In order to improve the achievable shift a fixed shunt inductance is also added. If a few additional elements are carefully placed, all the varactors can be controlled with a single control signal. By adding occasional boosting amplifiers, this system can be made arbitrarily scalable.

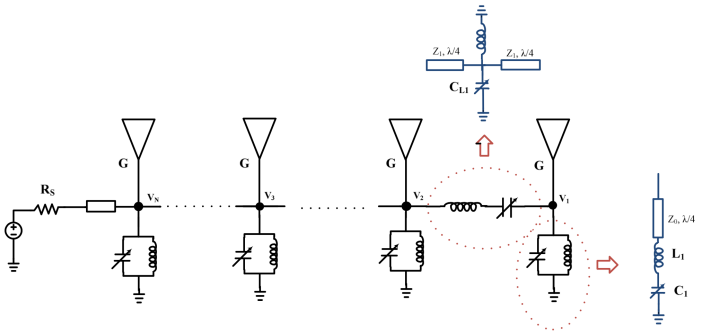

Fig. 3.3. Additions to extended resonance to allow a single bias voltage to control entire system [24]

In summary, the extended resonance technique can be used to combine phase shifters and power dividers into a single circuit. Modular, easily controllable systems can be created, offering the potential of substantially simplifying and somewhat decreasing the cost of phased arrays. Unfortunately, there are many applications for which it simply isn't suitable, because there is no way, without a large number of localized amplifiers, to provide a dynamic amplitude taper.

Vector Summation Technique

The struggle is always in maximizing array performance while minimizing cost, weight, spatial size, and other such factors. This section discusses many attempts to find the optimal balance, in order to provide a reference with which the work of this thesis can be compared.

By varying the magnitudes of two vectors, the vector which is produced when they are summed will have a varying phase. In fact, conisdering Vector A to have phase Theta, and Vector B to have phase Phi, if,

$$C = k_1 * A + k_2 * B \tag{3.3}$$

Then by adjusting k1 and k2, any phase between Theta and Phi can be achieved. This principle can be used to greatly reduce the number of phase shifters required in a system.

Many researchers have published variations of this technique for reduction of the number of phase shifters required in a system. The principle is that, based on the laws of vector summation, if two signals with different phases (but the same frequency) are added together, by varying the amplitudes of the signals, any desired phase shift between the phase shifts of the two original signals can be achieved.

In 2012, Daniel Ehyaie [10] proposed a system (see Figure 3.4 which, using only a single phase shifter, could achieve phase shifting for the entire array. For an array of N antennas, however, this design requires 2*N amplifiers (half of which have a variable gain) and N 3-dB couplers. Because it is a serial-fed array relying on the summation of an incident signal and reflected signal, the successive (per element) phase shift which can be achieved is:

$$\theta_{max} = 180 * a * sin(2/N)/\pi \tag{3.4}$$

Such a system as this requires only a single phase shifter, but needs a separate variable gain amplifier for each antenna. The operating steps are as follows:

1. Signal generator feeds into a 3dB power divider.

2. One output from power divider is phase shifted, the other is not.

3. Phase shifted signal is divided evenly among N different power combiners.

4. Original signal is divided and sent into N variable gain power amplifiers, each of which feeds into power combiner.

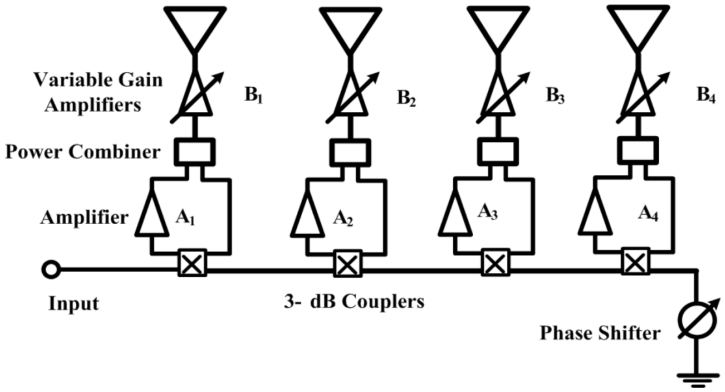

Fig. 3.4. Block Diagram of Ehyaie's Proposed Architecture

5. Shifted signal and amplified signal are combined in power combiner and input to antenna.

In summary, the vector summation method can vastly reduce the number of phase shifters in a system. It is extremely useful and will likely be a large part of future array technology. However, it has the disadvantage of requiring a total of 2*N power amplifiers, which must be considered when selecting the best option for a given application.

Arrays with Integrated Phase Shifters

[9] Proposes a "Scalable" array (see Figure 3.5) which, like many other designs, attempts to reduce the phase shifter count. It separates the array into groups called "subarrays" each of which has a only a single phase shifter. By cleverly feeding the input signal directly into one antenna, but passing through a phase shifter before it reaches the other antennas, and utilizing vector summation, it can achieve up to 33 degrees of scanning with an 8-element array (split into two subarrays). Like [10], however, it relies on a variable gain amplifier at each antenna in order to adjust the magnitude properly, and therefore does not bring down the system cost as much as could be desired.

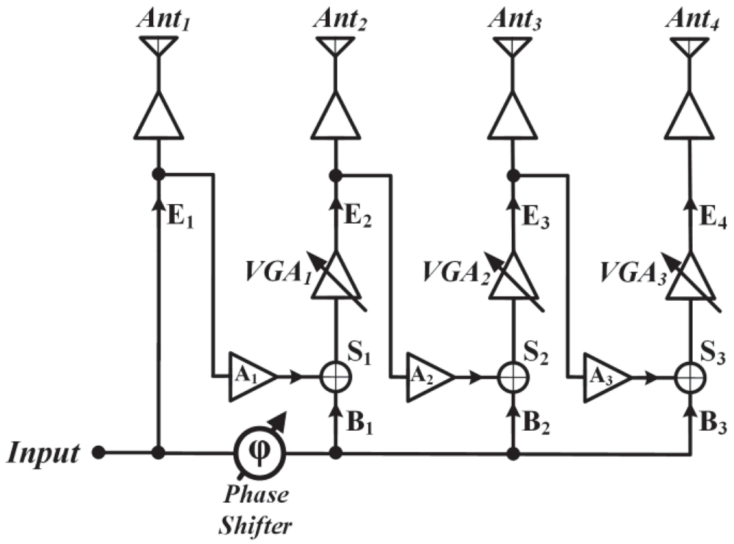

Fig. 3.5. Block Diagram of "Scalable, Simplified" Architecture

Massive MIMO Combining with Switches

Although the only considered application is data transmission, [27] proposes a method for decreasing the number of required "RF chains" (see Figure 3.6), by switching which chain, including (fixed, non-tunable) phase shifters, amplifiers, etc., supplies which antenna. By switching, fewer chains are required because each antenna has some lag time. The following figuring illustrates the scenario.

This is certainly interesting, but for many applications within wireless power, the arrays cannot afford to "take time off".

3.2 The Variable Power Divider

A key part of this thesis uses a variable power divider to "divert" appropriate power levels to the correct places in a phased array. These variable power divides have been researched in many various forms, some of which are discussed here.

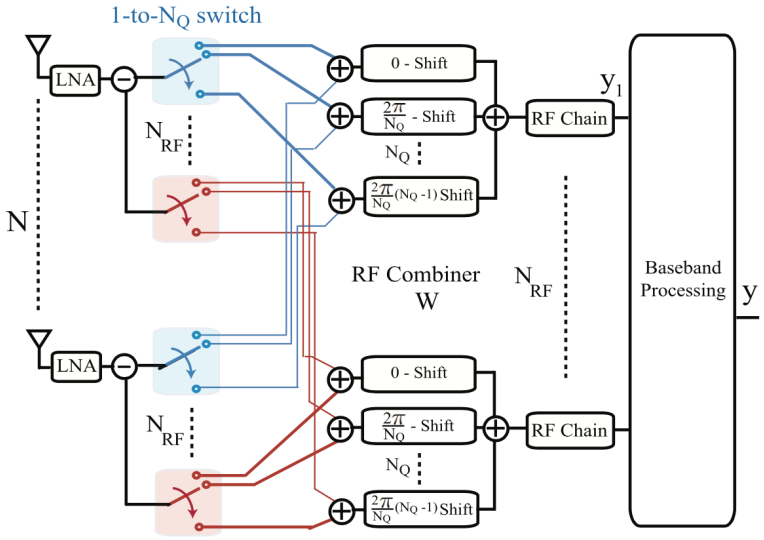

Fig. 3.6. Block diagram for Massive MIMO Combining System [27]

5GHz Transformer Based CMOS Variable Power Divider

[26] Uses a transformer and small RLC network (see Figures 3.7, 3.8) to achieve continious power dividing ratios from about -6 dB to +3 dB simply by the variation of a control voltage from -.5 to +.5 Volts. It is a simple, low cost method which could be useful for some applications, but unfortunately, the resistance of the diodes and conductor resistance of the transformer results in approximately 35 percent loss of input power. Therefore it is an excellent option for certain applications in communication systems, but not for wireless power transmission, where efficiency is obviously critical.

Unequal Wilkinson Divider with Variable Ratio

The Wilkinson Power Divider, as previously discussed, is a standard component of many RF systems, but is generally fixed in dividng ratio, and therefore does not provide oft-required flexibility.

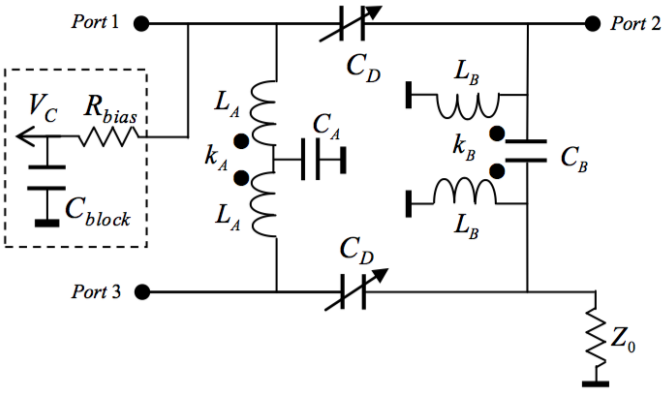

Fig. 3.7. Schematic of Integrated Transformer Variable PD in CMOS [26]

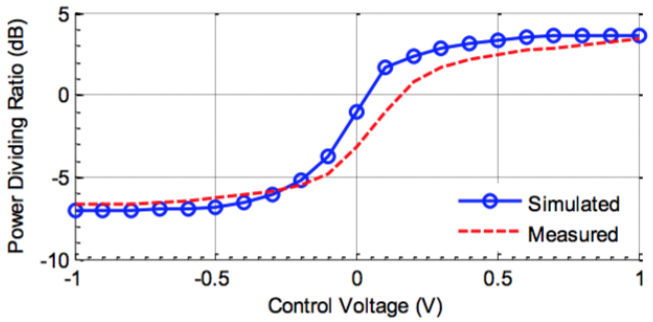

Fig. 3.8. CMOS VPD Power dividing ratio vs. control voltage [26]

[31] Proposes a Wilkinson Power Divider which uses a Defected Ground Structure (DGS) (see Figure 3.9) to vary transmission line impedances. This difference in impedance varries the power dividing ratio, and, through the adjustment of control voltage from 0-10V, the ratio can be change from 3:1 to 10.5:1. It is of a somewhat different nature than the other technologies described in this section, and it should be the topic of much future research. This device, however, has the disadvantage of only being tunable in one direction, whereas some others considered here can achieve dividing ratios significantly less than 1 if desired.

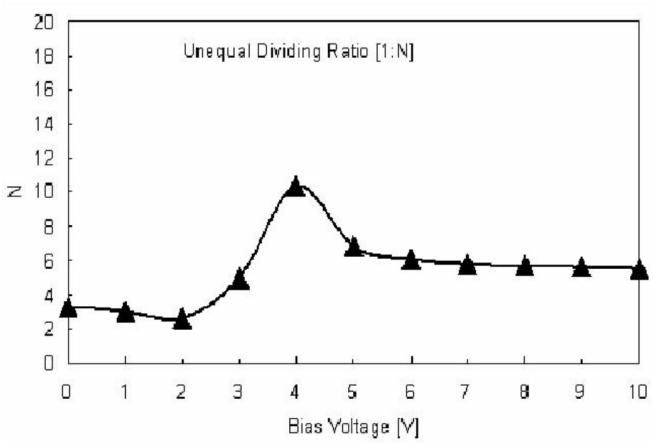

Fig. 3.9. Unequal Wilkinson Power dividing ratio vs. control voltage [31]

Varactor Based Variable Power Divider

[29] Uses hyperabrupt varactor diodes (varicaps) to provide a capacitive impedance on a transmission line. By changing a control voltage, this impedance can be varied, accordingly changing the dividing ratios. It is elegant in both its simplicity and utility (Figure 3.10).

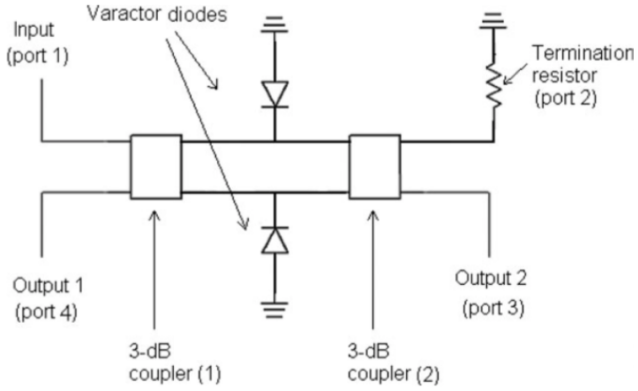

Fig. 3.10. Schematic of varactor based divider [29]

Additional Varactor Based VPD

[34] Describes another varactor diode based VPD (Figure 3.11), possessing very similar nature to that of [29], with two "3 dB Hybrid Couplers" and two varactor diodes making up the bulk of the device. This device is discussed here for two reasons:

1. It is unique in that it is designed to operate successfully at both 2.4 and 5.8 GHz.
2. The tremendous tunability of the output power dividing ratio makes it the best option for use in this thesis.

Although there is some unexpected behavior at very low applied voltages, above about 2 Volts (for 2.45 GHz) the device behaves as an increasing function. In linear scale (once again, looking at the 2.45 GHz band), the power dividing ratio can vary from 1:50 (0.02) all the way to 100:1 (100) as the applied voltage is changed from 2 to 25 Volts!

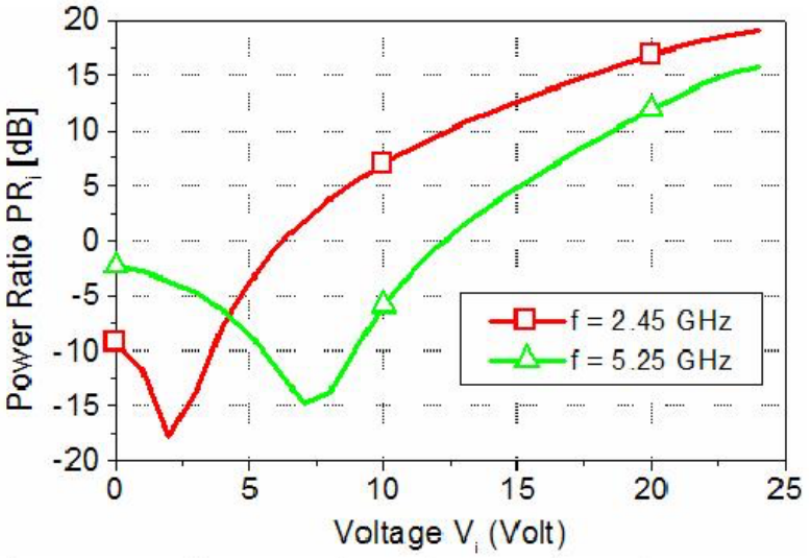

Fig. 3.11. Dividing ratios with applied DC voltage [34]

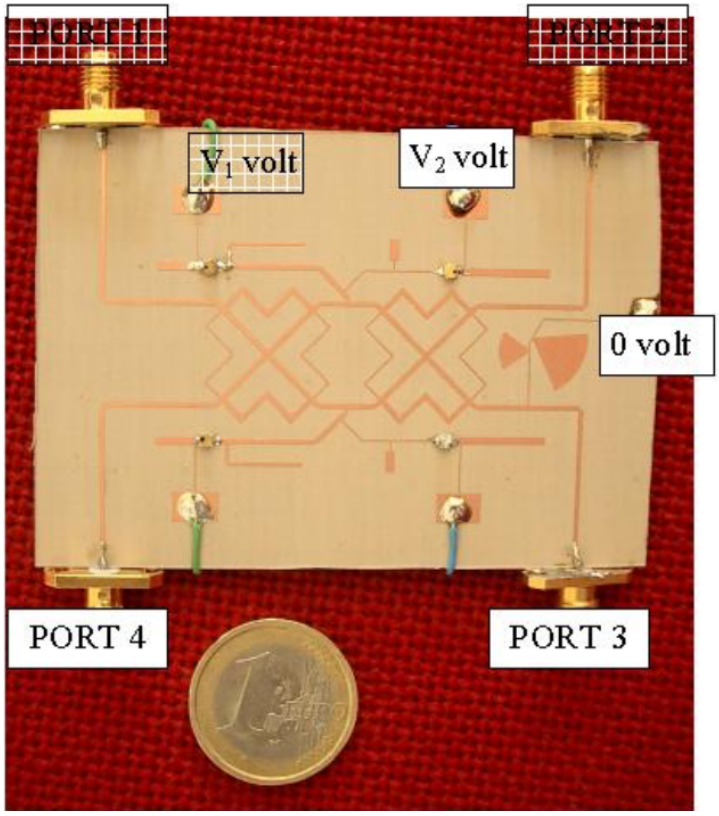

Fig. 3.12. VPD PCB clearly shows locations of pads where tuning voltage (V1,V2) can be applied for separate operating frequency bands [34]

PIN Diode VPD

[53] Details a variable directional coupler (equivalent functionality to power divider) which relies on the DC voltage-controlled variable impedance of a PIN diode which terminates the normally coupled port to achieve dynamic splitting (coupling) properties. Figure 3.13 shows the extreme simplicity of the circuit.

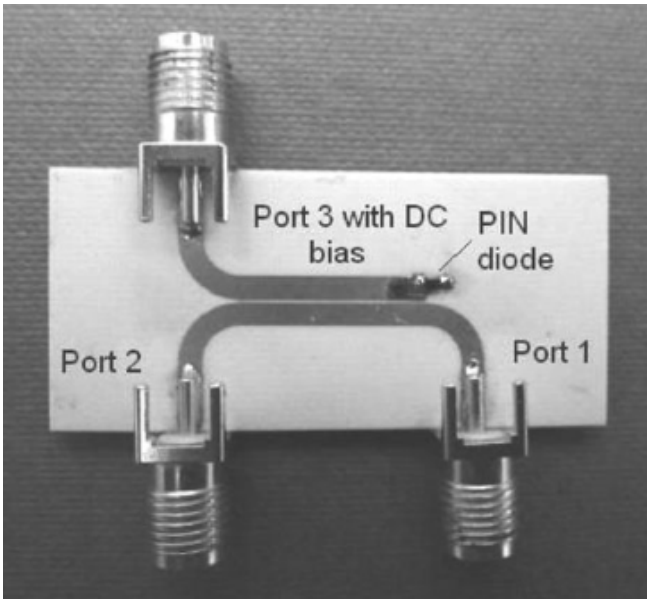

Fig. 3.13. PIN Diode-based variable directional coupler [53]

3.3 Microwave Wireless Power Transfer

Space Solar Power

"Space Solar Power" is the idea of putting solar cells in space (where they gain exposure almost without interruption all day and year round), inverting the DC power, and using high gain antenna arrays to "Beam" the power back to earth [38]-[42]. Among the most popular system proposals is that of a "sandwich module", which would contain in a single package, a solar cell array for power harvesting, power electronics for DC-RF conversion, and an antenna array for power transmission [41][42]. The goal of this thesis is to make this, and many other applications potentially more attainable, primarily by means of cost reduction.

Hexagonal Phased Array for WPT

[1] Discusses a hexagonal antenna array of 6000 x 6000 elements with .8 lambda spacing, at 2.45 GHz. The primary goal was to achieve arbitrarily low sidelobes for applications such as Space Solar Power. With the employment of a Chebyshev taper, the sidelobes were successfully reduced to a level of -240 dB below the main beam (which was itself 160 dBi). This is shown in Figure 3.14.

Although the choice of 0.8 lambda strikes an excellent balance between low sidelobes and high gain, it is not suitable for some applications because of the issue of grating lobes. Grating lobes, sometimes equal in magnitude to the main lobe, can appear when the elements are spaced more than 0.5 lambda apart. These could pose a substantial safety risk at high power levels, and tend to present themselves with increasing magnitude as the beam steering angle is increased. They may be (or may not be) very small when the beam is perfectly broadside, and are often hidden to a 2-dimensional cut of the radiation pattern.

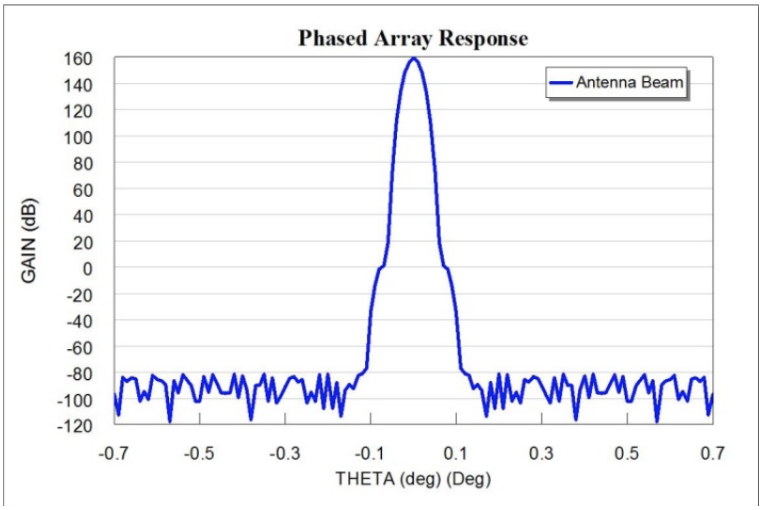

Fig. 3.14. Radiation pattern showing low SLL in large hexagonal arrays [1]

Low-Medium Power UAV Charging at Low-Mid Range

In 2017, a team from Nanyang Technological University in Singapore published a paper [43] on low-mid range (1 to 4 meters) charging of a UAV at low-medium powers. The designed receiving / rectifying module was lightweight (500 grams in total), and would therefore be appropriate to mount on a UAV. The transmitter used was a horn antenna with gain of 16 dBi. Although the recitfier which was designed and used has remarkably low efficiency (46.5 percent maximum), it is certainly valid that low cost applications would require low cost parts, and this may, therefore, be an accurate representation of what could be expected. Results are shown in Figure 3.15, Receiver is shown in Figure 3.16.

R (m)	P_t (W)	E-field (V/m)	Max Charging Current (mA)	Max Charging Power (W)	P_{theo} (W)
1	323	301	190	2.28	10.49
2	430	354	50	0.6	3.49
2	133 (threshold)	194	20	0.24	1.08
4	173 (threshold)	161	8	0.096	0.35

Fig. 3.15. Power received vs. transmitted results from Singapore publication

The results here are not encouraging. The best result achieved in any of the test, at a distance of 1 meter, still results in a power efficiency of about 0.7 percent. If this is blamed partly on the low efficiency rectifiers and voltage regulators on the receiving end, and these are assumed to be lossless, the efficiency at 1 meter becomes only 1.9 percent. This is discussed because it is important to realize the types of efficiencies which are achievable with small arrays such as the one used in this study. In order to acheive better results, arrays of substantially more elements must be used.

MM-wave WPT rectenna circuit

[14] Details an on-chip harmonic-rejecting antenna, shown in Figure 3.17, which operates at 160 GHz, in the millimeter-wave range. It states “At present, most reported rectennas are designed to operate below 30 GHz. However, for space-to-space WPT applica-

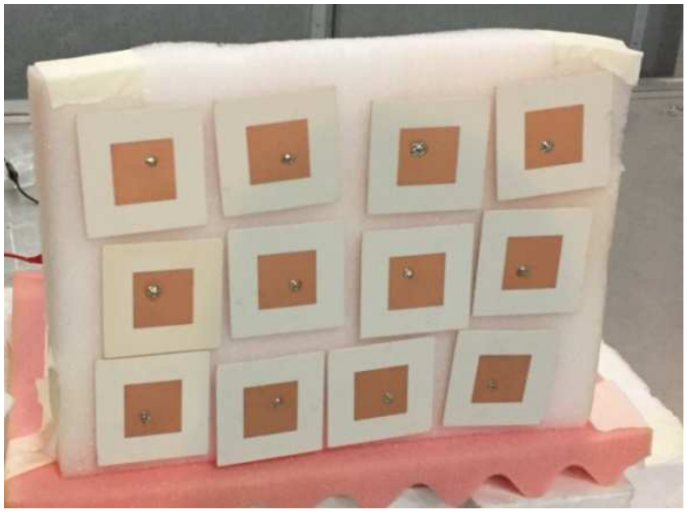

Fig. 3.16. Receiving Array Used in low-medium power WPT system

tions, rectennas operating at mm-wave frequency have the advantages of compact size and a higher overall system efficiency than those of low-frequency rectennas." These statements and more make it a very intriguing topic. The topic of rectenna design, especially at such high frequency, is an almost untapped field, and therefore the work done in this paper is both exceedingly complex and brilliant.

They have designed a harmonic-rejecting antenna which alleviates the need for an external low-pass filter to be connected. The goal of the device is to keep harmonics of the primary frequency from entering the device, potentially re-radiating and decrease device efficiency. Connected to this antenna is, built into the same piece of Silicon, a CMOS rectifier, which eliminates the external rectifier from the system design. All of this decreases insertion loss and enhances performance.

Although the receiver side of the wireless power transmission problem is not heavily considered in this thesis, papers like this are extremely useful for considering system design. Namely, the existence of a rectenna at such a high frequency (which had never been done before), and the knowledge that it has the potential to offer even greater efficiency than standard bands, plays heavily into the operating frequency chosen on the transmit-

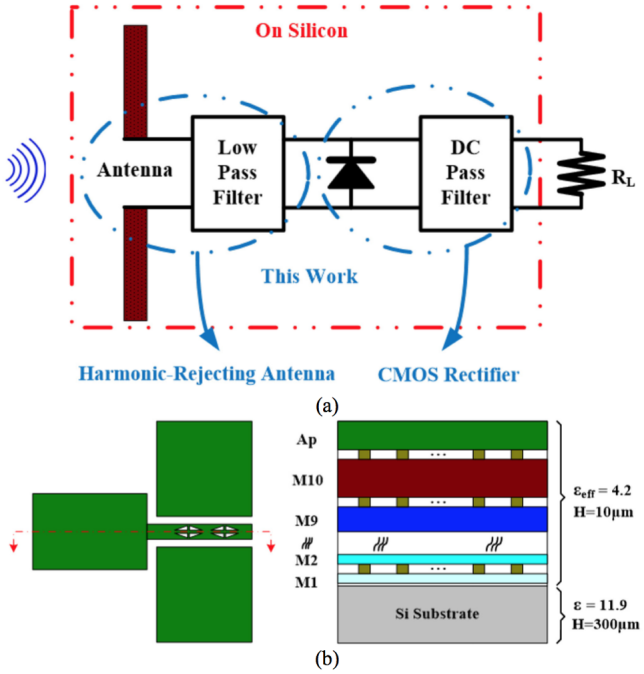

(a) Schematic of a traditional rectenna circuit. (b) Top view (left) and cross-sectional view (right) of the proposed on-chip harmonic-rejecting antenna.

Fig. 3.17. MM-wave on-chip antenna with built-in filter and rectifier, compared to traditional rectenna

ter side. Unfortunately, the technology does still need development: Only extremely small power levels were considered in this paper (less than 1 mW), but the peak power conversion efficiency comes in at 8.5 percent (See Figure 3.18).

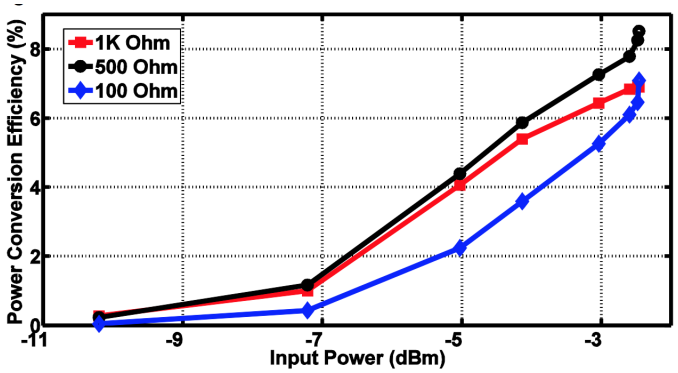

Fig. 3.18. Power conversion efficiency of rectenna system

Small Patch Arrays for 5.8 GHz WPT

[13] Conducts a study of wireless power transmission efficiency at 5.8 GHz with patch antennas. Although virtually no "novel technology" is presented, it does give a good baseline for what effieincies are acheived by some existing systems. Two sizes of virtually the same system are studied: one with 6x6 transmitter and 4x4 receiver (pictured in Figure 3.19), the other with 8x8 transmitter and 8x8 receiver.

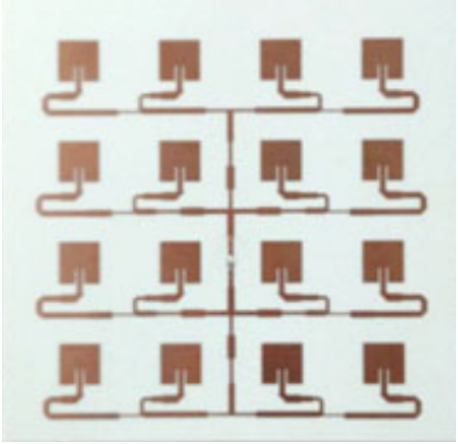

Fig. 3.19. One of arrays used for short range microwave WPT system [13]

The system setup with smaller arrays achieved efficiency of approximately 38.4 percent, while the larger arrays had improved performance of about 46.9 percent. It is instructive to know that these reasonable conversion efficiencies can be obtained (albeit at small distances) with extraordinarily low cost, low complexity systems. This is a good sign for the future of the technology.

4. AUTHOR'S CONTRIBUTION: FEEDING ARCHITECTURE RESULTS

4.1 Introduction

There are many applications where it would be desirable to send power to many different targets at once; This could be the charging of mobile robots as they drive around in a warehouse, it could mean sending destructive power to damage hostile drones as they fly into a football stadium and begin to fire on people, or any of many other possible examples. There are some technologies today which can successfully jam or destroy drones [32][33], even some that can do it very quickly, but there are none the author is aware of which can "take down" an entire fleet of drones simultaneously. Much research has also been done for microwave / millimeter wave wireless power transfer, and much more has been done for wireless charging of other kinds, such as inductive and magnetic resonant, but the author is not aware of any systems such as the one proposed here. More than anything, this system is special because it can adapt instantaneously to any number of targets (within limits), and needs no setup or design in advance to "guess" how many receivers there might be. Additionally, it has the "dual use" of also performing location positioning of the receivers.

4.2 Novel Dual Use Reconfigurable Array

Proposed is a large antenna array which can split itself into many separate "subarrays", each one behaving as a separate system, and transmitting power to an individual target. It is important to realize, however, that there is no physical separation taking place. The levels at which each antenna is amplitude tapered and phase shifted are the only things that actually change when the array "splits". This can be visualized in Figure 4.1.

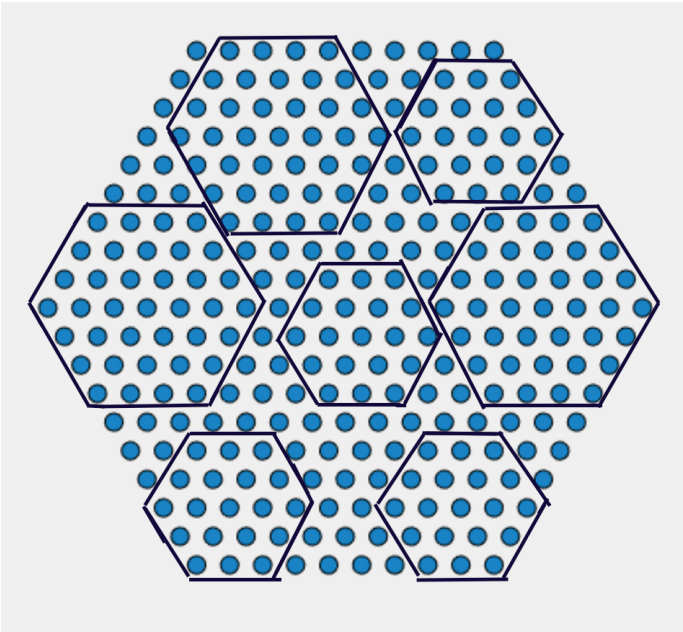

Fig. 4.1. Division of system into 7 smaller subarrays

This thesis proposes a phased array which operates based on the following steps:

1. Select elements of the array are in “listening mode”, determining location information about the targets (AGVs, mobile phones, enemy drones, etc.) via some method such as “Direction of Arrival” or Radar.

2. Based on the number of targets which appear within range of the array (take this number to be N), the array reconfigures itself into N subarrays. Some elements remain in listening mode.

3. Each of these subarrays is assigned to transmit to an individual target, and each must utilize whatever amplitude taper and phase shift is required for beam steering. CPU provides all necessary signals to amplifiers and other elements.

4. Because the array is composed of dual-band or wideband antennas, in a commercial application where the targets can send beacon signals, no particular antenna has to be assigned to be a permanent receiver or transmitter. Instead, the array can adapt as needed,

using dormant elements as listeners, which can operate on a separate band from the transmitting elements in order to provide the CPU with updated location information and adjust its excitation accordingly.

5. Process continues as locations and number of targets change.

This array has many potential applications. It could be used for transmitting power wirelessly to robots or AGVs in a warehouse, allowing an increase in time between battery recharges. It could send damaging amounts of power to disable enemy drones. Or, it could allow a store to monitor the locations of guests who have downloaded the "mobile app". The app could send out a "beacon signal", and the array could track and even send coupons and other marketing messages to the customer, and perform data analytics on them–all without them being connected to the store Wi-Fi network.

It is valuable to envision this "4-Bus Method" (Figures 4.2 and 4.3) as compared with both "classical" (Figure 4.4) and other modern methods–namely, that proposed by [10], which is shown in Figure 3.4.

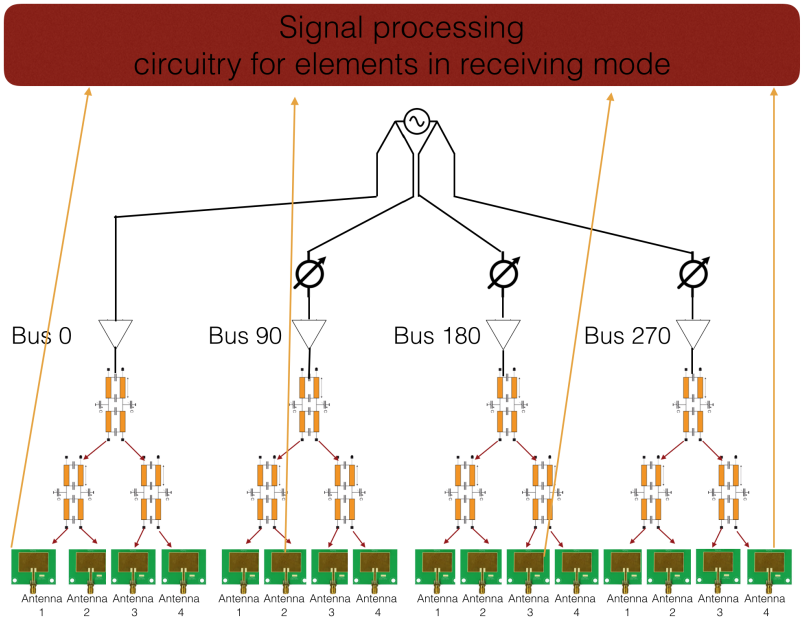

Fig. 4.2. Simplified Block diagram of Proposed "4-Bus Method"

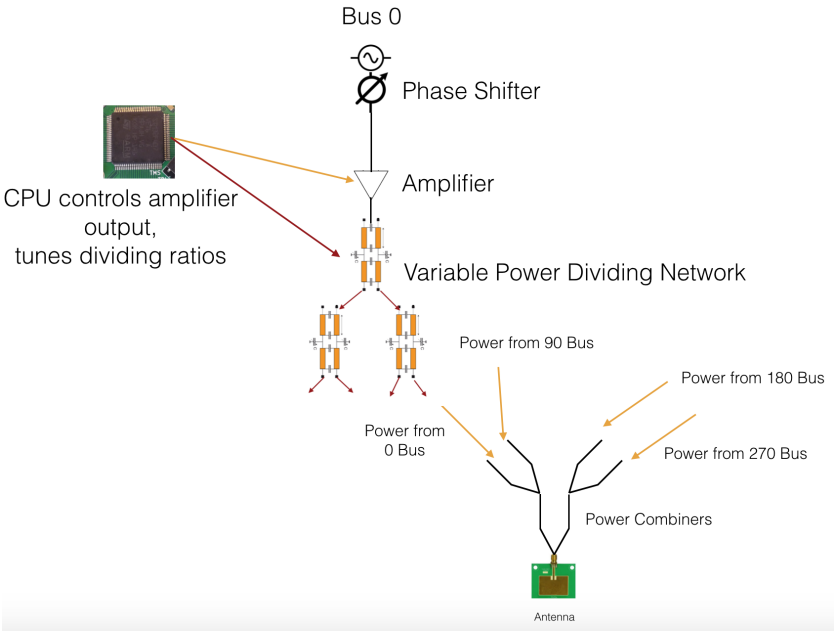

Fig. 4.3. Diagram of a single antenna and single bus of the "4-Bus Method"

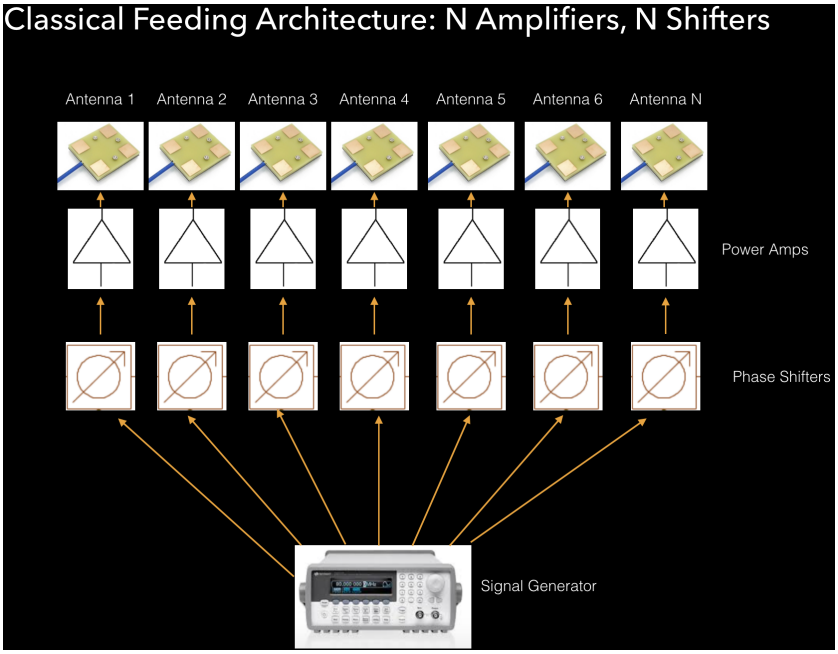

Fig. 4.4. Block Diagram: "Classical" Feeding Architecture

4.3 Discussion on Array Operation

This reconfigurable array works as follows. The array is in place, awaiting instructions from the CPU, and perhaps performing some operation in attempt to recognize and locate receivers or targets (see Figures 4.5, 4.6, 4.7).

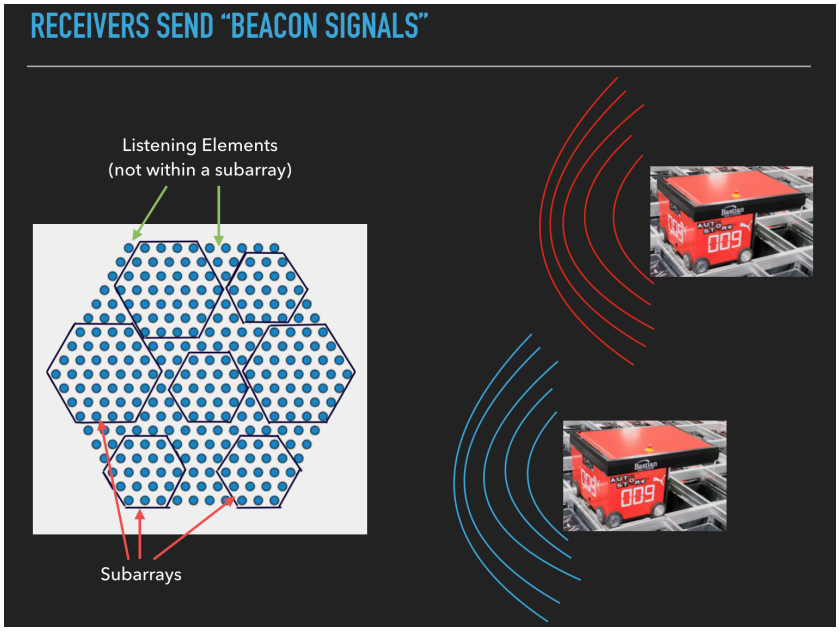

Fig. 4.5. In mobile robot charging applications, beacon signals may be sent

When the CPU determines, either by an external radio communication, or through the Radar or "Direction-of-Arrival" operation of the array, that there are receivers which should be powered, the array separates into the appropriate number of subarrays. Other methods that could be used to interpret position from the beacon signals are "Time-of-Flight" and "Retrodirectivity". The exact circuitry that would be required for each of these methods would differ in each case, and therefore it is not treated specifically, but lumped generally under the "signal processing" block. It is also key to note that, for an array which utilizes dormant elements for positioning, there must be a switch at the connection to each antenna, which allows it to change between receiving and transmitting modes, as shown in Figure 4.6.

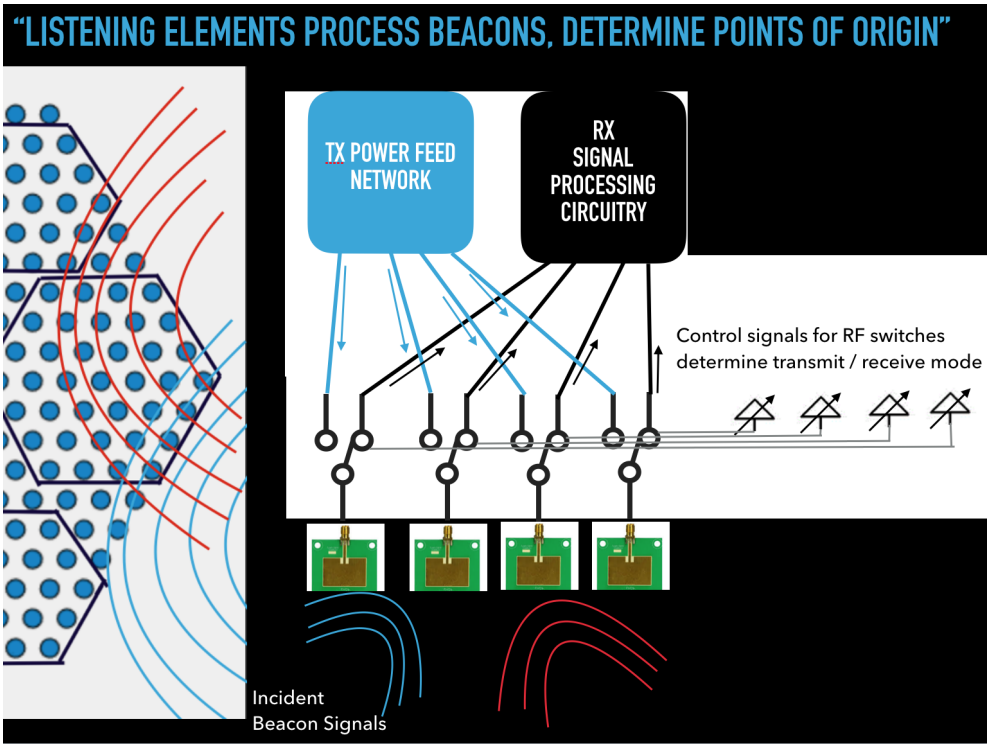

Fig. 4.6. "Listening Elements" perform positioning using "Direction-of-Arrival", "Time-of-Flight", "Retrodirectivity", or another method

Returning to the "separation of the array into subarrays", this separation does not occur through any physical mechanism, but rather, the varying excitation of the constituent elements causes multiple, separately directed and controlled beams, to result, instead of one large beam (see Figure 4.8). Depending, once again, on the application, these "subarrays" may be separated by a row or column of dormant elements which could be used to provide continuous updates on target positions. If ever the receivers change position such that the beams from the subarrays begin to cross over each other, these subarrays can simply switch, each taking responsibility for powering the opposite receiver. Finally, it should be noted that in some cases, a termination resistor or cheap absorbing block may need to be added, in order to eliminate reflections and interference from power incidentally reaching an open switch.

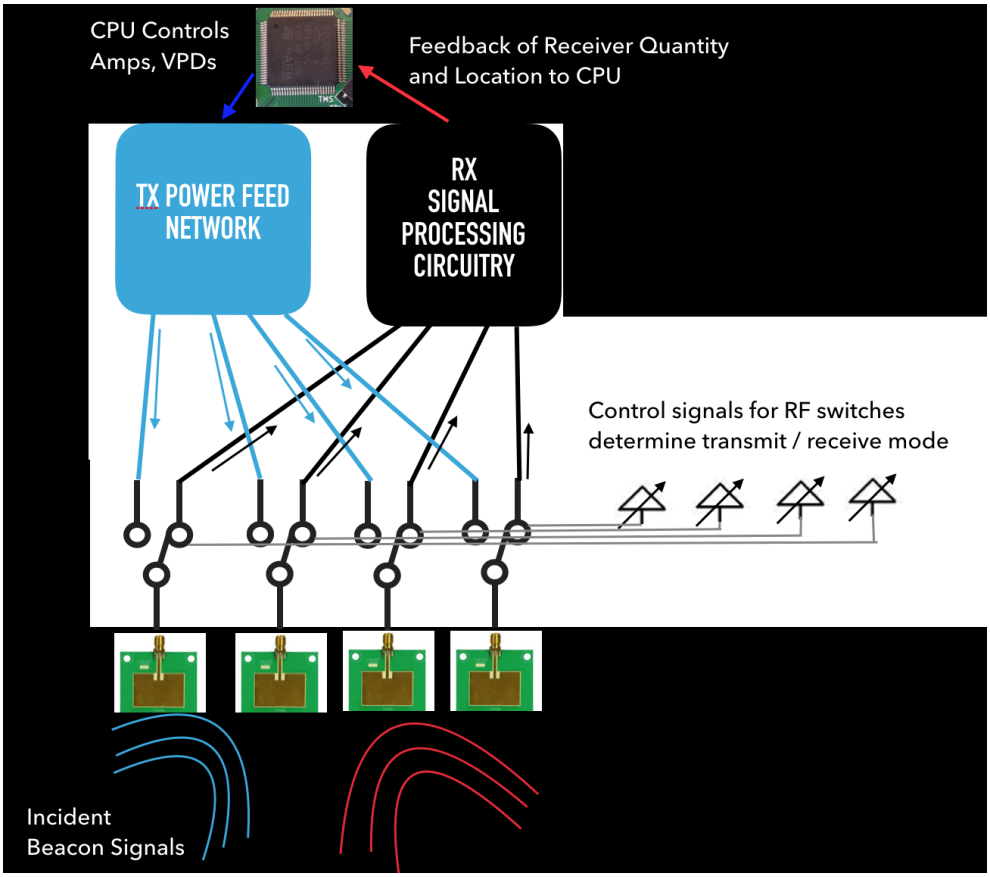

Fig. 4.7. Flow of information and power: State of switches determines whether antennas are in transmit or receive mode

There are probably a few questions that arise in the mind of the reader at this point. Namely:

1. How does the partitioning of the array into subarrays affect efficiency of power transfer? That is, how does the decrease in the size of each array affect it?

Of course, the decrease in size of each subarray will decrease power efficiency. An intensive study is performed in a later chapter which examines this issue and produces some useful results and approximations for understanding it quantitatively.

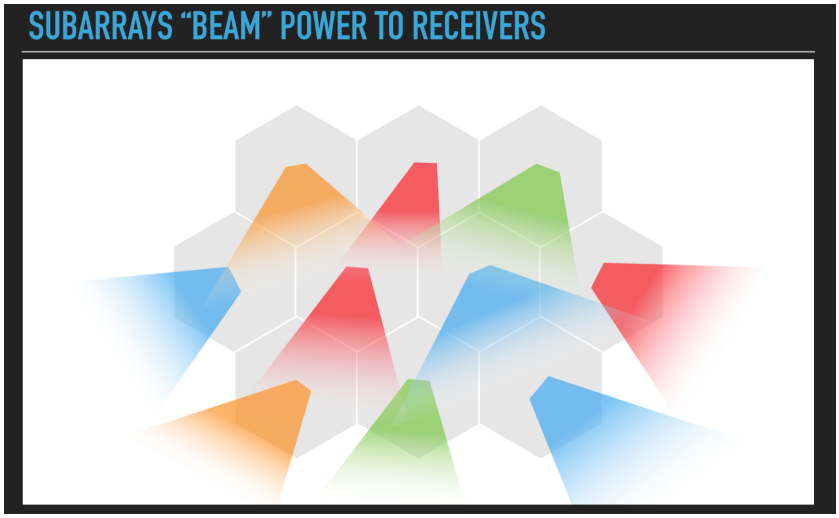

Fig. 4.8. Subarrays beaming power to individual receivers

2. Will the power and positioning signals interfere with each other?

They would certainly interfere with each other if they were operated at the same frequency, but antennas could be selected for the array which possess reasonably large bandwidth. The operating frequency for the positioning system could then be chosen at the other end of the antenna bandwidth from the power signals.

3. What happens if the array is powering multiple receivers, but then some leave the area, or several more enter it?

The system is fully dynamic, and can adapt to changes in extremely short time periods. Because the array always configures itself to have the same number of subarrays as there are receivers to power, if the number of receivers goes down, the array turns off those subarrays, and then absorbs the excess space into the other subarrays, to make them larger. Or, alternatively, the array entirely reconfigures itself, creating a totally new network of subarrays which are larger than the previous ones (because there are fewer of them). When the number of receivers increases, the process is reversed; That is, more subarrays are needed, so the CPU must reconfigure the subarray network to make room for the new ones.

4. What about safety issues, and compliance with regulations such as those of the FCC and FAA?

It is clear that both the power level of the application and the environment in which it is being used are key considerations. This is not the focus of this thesis, but if regulatory bodies stand in the way of the use of these technologies in uncontrolled environments, there are many ways in which they could still be used, if proper precautions were taken to separate the dangerous energy levels from exposed humans.

5. What array architecture / feeding method will be used?

This is one of the key points of this thesis, and has its own devoted section below.

6. What steps must be taken by the system in order to perform all this?

The following is the "order of operations" for the array:

A. Target location information is given to the CPU.

B. CPU determines required number of subarrays, assigns appropriate phase shift and amplitude values.

C. Amplifiers and phase shifters are assigned required values.

D. Charging or damaging power is supplied to all targets simultaneously.

E. Repeat.

An earlier section has discussed in detail the issues of phased array beam steering, gain, power density, etc., so we will not cover it again here. There are two important questions consider, however, in order to really understand how the system works: How can the system excite each antenna properly in order to achieve the beam steering and tapering required, and how can we predict or measure power density / power efficiency? Fielding these questions in order, we begin with a detailed discussion of the proposed "4-Bus Feeding Architecture."

4.4 4-Bus Feeding Architecture

What is required is a way to dynamically control the amplitude and phase excitation at each antenna without a localized power amplifier or phase shifter. Based on the work from [10], it was determined that the best way to do this is via the combination of variable proportions of signals with different phase shifts. In [10], however, a variable gain amplifier at each antenna was used to provide this flexibility, and the nature of the feed severely limited the achievable per element shift. In the proposed "4-Bus Method", the use of 4 parallel buses with parallel feed [8], instead of 2 with series feed, allows any phase shift which could be required.

How Does it Work?

The guiding principles for the system are based on the laws of vector summation, as demonstrated in [10]. [10] used power combiners to add two signals of different phases, tuning their proportions with a variable gain amplifier at each antenna. This allowed a single phase shifter to serve the entire system, but severely limited achievable steering angle, and did not solve the issue of amplifier count.

The proposed "4-Bus method" takes the output signal from its function generator and splits it four directions. In each direction, there is a phase shifter which shifts to either 0, 90, 180, or 270 degrees relative to the original. These signals are amplified appropriately, and then enter a large network of "variable power dividers", a relatively unknown device which was discussed in an earlier section[26][29][31][34]. The premise of this device is that, by adjusting a variable analog DC voltage input, the ratio between the power outputs at the two output ports can be tuned. That proposed in [34] can achieve any dividing ratio between 1:50 (0.02) and 100:1 (100), which is the performance we will assume the "VPDs" used in this thesis to be capable of.

Each antenna in the system which is not in "dormant mode" has an amplitude and phase value which it requires in order for the system to achieve the tapering and beam steering it needs. If this phase angle for a particular antenna were 45 degrees, the CPU would determine that it needs power from both the "Bus 0" and "Bus 90", in equal quantities (where the quantities are amplitude times cosine of the angle, and amplitude times sine, respectively). If the phase angle were 300 degrees, the antenna would need power from "Bus 0" and "Bus 270", in unequal amounts which would depend on the required amplitude. It is clear, however, that any amplitude and phase can be achieved by proper combinations of power from a select two of the buses.

In order for such precise quantities to be supplied at each antenna, the CPU carefully tunes the dividing ratios at each of the many, many VPDs, so that just the right amount of power from each bus reaches the antennas (for each antenna, there will be two buses which don't need to supply any power). Therefore, the system operation could be summarized as follows:

1. "Dormant elements" or external radio listen for updates of quantity and location of receivers / targets.

2. When information is received, CPU tunes VPDs, updates amplifier power outputs (taking into account losses inherent to vector summation).

3. Separately shifted signals are amplified, pass through VPD network, are power combined together at each antenna, and radiate toward the assigned targets.

4. Some "listening" mechanism is continued in order to provide system with continuous updates about receiver quantity and location.

We categorize the following results into three convenient sections: Performance, cost, and "other".

Performance of 4-Bus Method

The primary weakness of the method is the inefficiency of the vector summation of various phases. That is, there are additional internal losses associated with the combination of the signals from different buses. The result of this is that more power must be input into the system in order to get provide the antennas with the same excitation. Repeated simulations show that the internal power efficiency is consistently very close to 78.5 percent.

On the brighter side, a unique (as far as the author is aware) figure of measurement for describing these types of systems is Resource Cost Effectiveness, or "RCE". We define this to be essentially a measure of how well the system uses all of its resources. That is, if the system only averages 1 Watt total power output when the sum of all its amplifier capacities is 100 Watts, the RCE is extremely low, only 1 percent. A small RCE is a sign that the system architect is spending large amounts of money without obtaining value from it, and it would be beneficial to increase this figure wherever possible.

In order to determine the RCE of the 4-Bus method as compared to classical architectures, a number of simulations have been run, and the results averaged. The system in question is a 20x20 reconfigurable rectangular array which uses at least two of its columns at any given time for location positioning. Taking the maximum amplitude or taper value to be 1 Watt, the maximum conceivable total power output at any time is 400 Watts. A Classical Architecture would need a 1 Watt amplifier at each antenna, totaling 400 Watts in total system capacity. The percentage of this value that is actually used is the RCE, and it, as well as system power consumption, is plotted (in Figures 4.9 and 4.10) against that of the 4-Bus method. Mathematically, RCE can be expressed as

$$RCE = ResourceUsage/SystemResourceCapacity \tag{4.1}$$

It may seem strange that the 4-bus method can possess superior RCE if it wastes a portion of its power. The explanation for this is as follows; The 4-bus method has internal losses, the result of which is that more power must be input into the system in order for the desired amount to emerge on the other side. However, because of the nature of the system,

Fig. 4.9. Power Consumption Shows Losses Inherent to 4-Bus Method

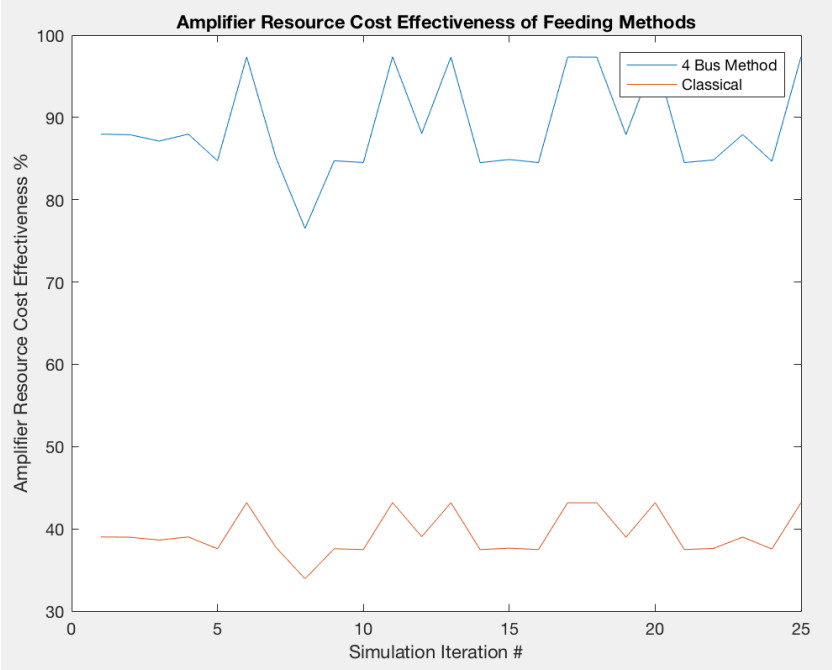

Fig. 4.10. In spite of internal losses, 4-Bus Method has much better RCE

it is not necessary to purchase superfluous amplifier capacity which will rarely be used, as is frequent in the classical architecture. That is, the 4-bus method allows the system architect to only purchase what is needed, and no more, which results in a huge upfront cost savings, as will become apparent later.

It is valid to question what would happen if ever it was necessary to pass all of the power incident upon the VPD to a single one of its output ports. The ”infinite dividing ratio” exceeds the capabilities of the device. In some applications, the result of this could be disastrous: Wrong proportions of power would result not only in amplitude error, but also significant phase shift error at many antennas. This could lead to the beam being directed altogether in the wrong place, ending in total failure of the system operative goals or large safety and interference issues.

In order to prevent this, an update (See Figure 4.11) is proposed which utilizes a “bypass junction” built out of simple RF switches. In this junction, there are three parallel paths. One path allows all the power to “bypass” the VPD and proceed straight to port 1, while another path allows ”bypassing” directly to port 2. Finally, the power can be fed into the VPD as usual, the dividing ratio being tuned by a separate control voltage. This update reduces feed network error substantially, as shown in Figures 4.20 and 4.21 for an example discussed below. It is also worth noting at this time, that a special connector or “Balun” may be necessary at the input of the variable power dividers–likely a simple coax to microstrip line connector. Because many of the VPD devices which have been considered already have this built-in, it is assumed to incur no additional cost, but is included in the system diagrams because it is a necessary component which may not always be built-in.

This “bypass” concept was tested and verified with actual hardware. The test system block diagram and practical test setup are shown in Figures 4.12 and 4.13.

The switches were test with their various configurations, and the received power (with expected insertion losses calibrated out) was recorded and compared to expected results. Results are shown in Figures 4.14 and 4.15. Additionally, the BOM for this setup can be found in the Appendix.

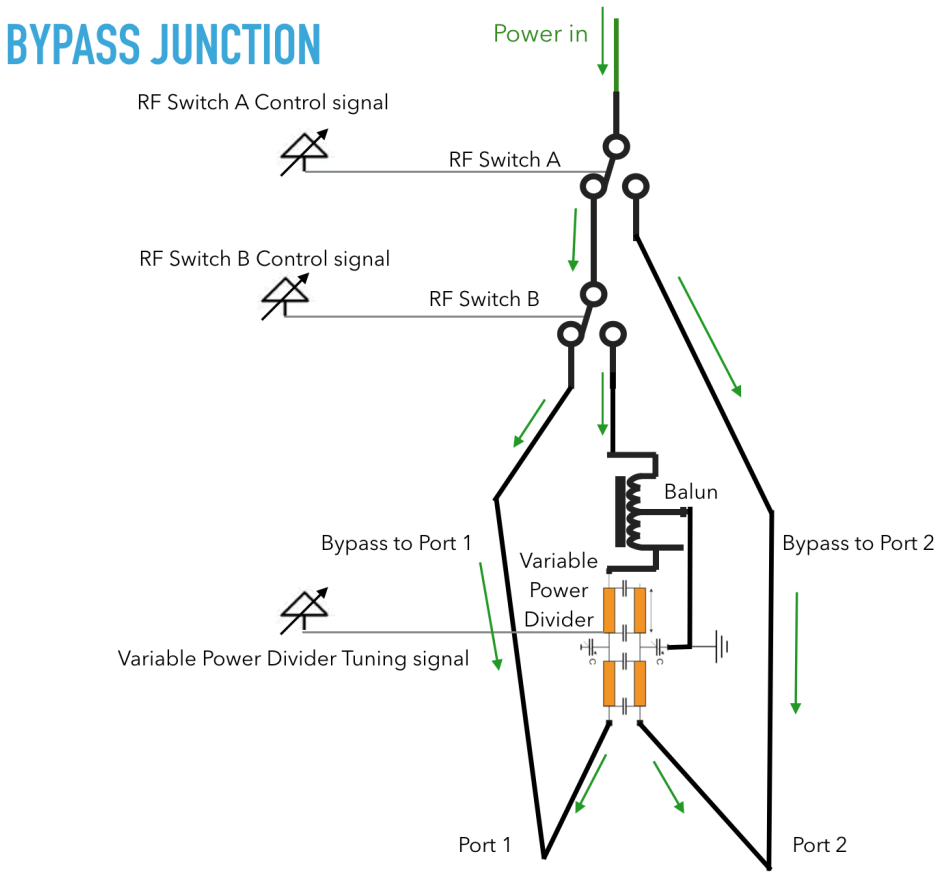

Fig. 4.11. Control circuit allows "bypassing" of all power to a single port, or power division to both

A few notes of explanation are necessary: This mode of the spectrum analyzer lacked a proper reference. That is, although the qualitative results shown were correct, 35 dB must be added to the the value shown to yield the actual value in dBm. In regard to the table presented–For the "Power Expected" value, a range is provided because of the tolerance of manufacturer insertion loss specifications. For the column discussing the Δ between received and expected power, the "midpoint" within this range is used. All results were very reasonable, and demonstrate via a very simple test that this bypass junction is a valid method for diverting power within a feeding network.

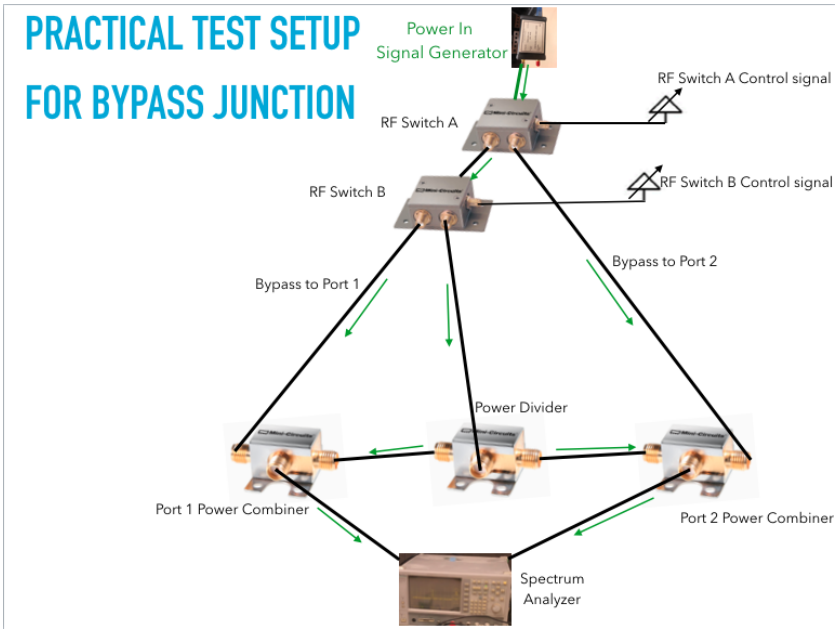

Fig. 4.12. Power combiners allow convenient power measurement at each port without unplugging additional wires for each test

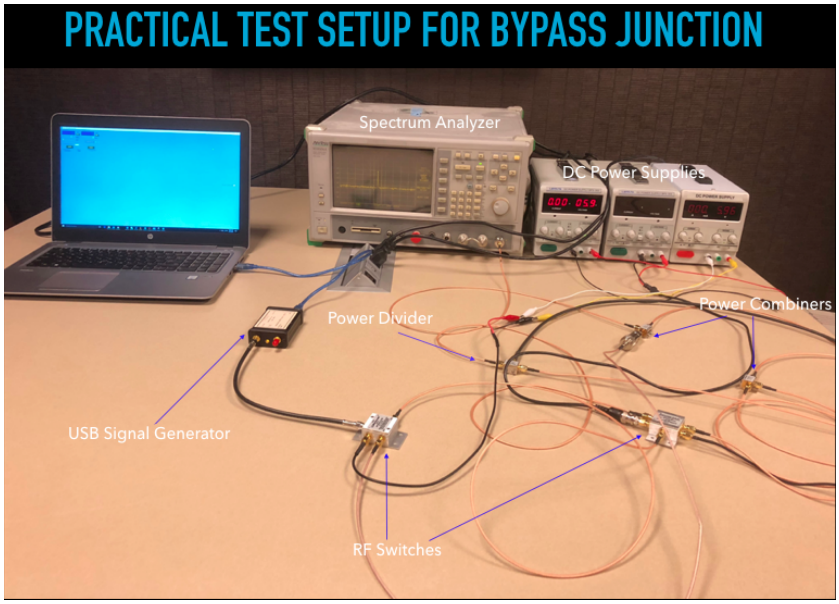

Fig. 4.13. Practical Test Setup

To determine what success can be obtained with this newly invented “bypass junction” in a phased array system, we must first understand the result without it. A rectangular array of 6 x 3 elements (shown in Figure 4.16) with half wavelength spacing, separated into two

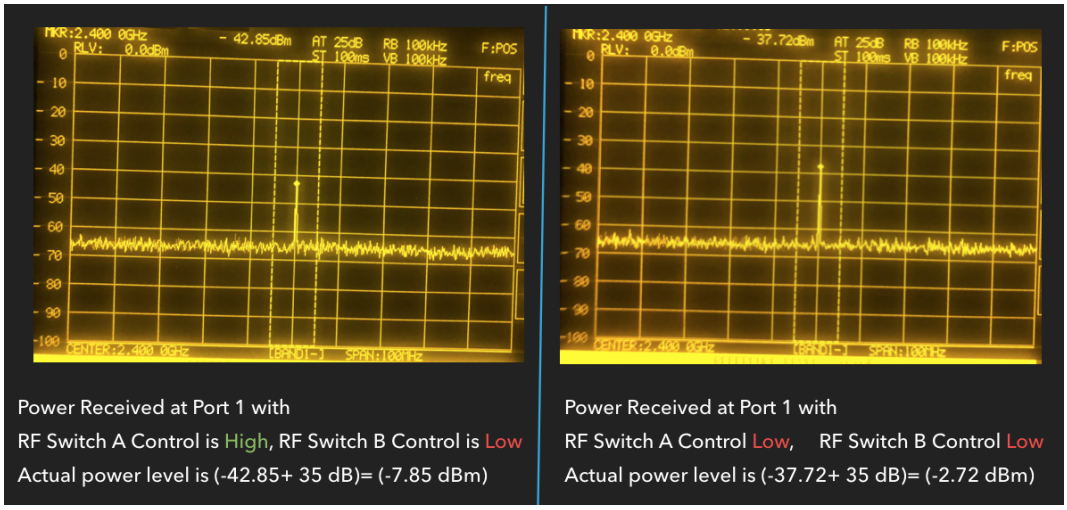

Fig. 4.14. Spectrum analyzer shows power delivered to Port 1 for various HIGH-LOW and LOW-LOW switch configurations

TEST RESULTS FOR BYPASS JUNCTION AT 2.4 GHZ

Control RF Switch A	Control RF Switch B	Port 1 Power Received	Port 1 Power Expected	Port 1 Δ of Received, Average Expected	Port 2 Power Received	Port 2 Power Expected	Port 1 Δ of Received, Average Expected
HIGH	-	0 Watts	0 Watts	0 dB	~ 0.7 dBm	0.7 dBm < Pr < 3.0 dBm	1.15 dB
LOW	HIGH	~ -7.85 dBm	-10.1 dBm < Pr < -5.5 dBm	0.05 dB	~ -7.89 dBm	-10.1 dBm < Pr < -5.5 dBm	0.09 dB
LOW	LOW	~ -2.72 dBm	-3.4 dBm < Pr < 0 dBm	1.02 dB	0 Watts	0 Watts	0 dB

Fig. 4.15. Power Results from Bypass Junction

"subarrays" is considered. Although this is much smaller than most which would be used in such applications as this, it allows ample illustration of the issues at hand without needless complexity.

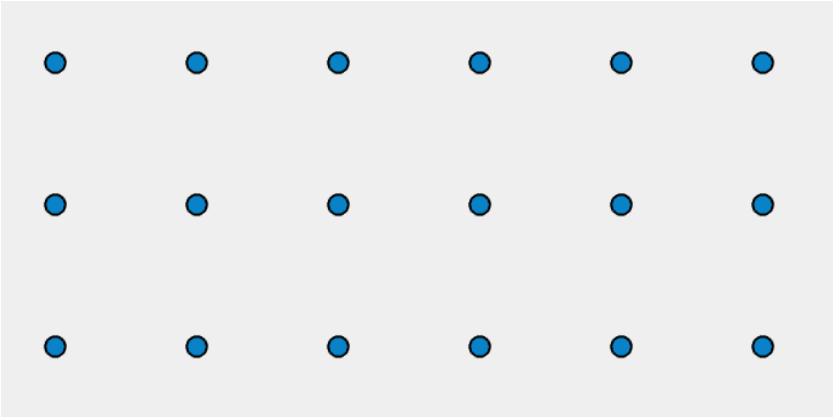

Fig. 4.16. Layout of small, simple 6x3 rectangular array

Taking the receiver assigned to subarray 1 to be at a steering angle of 37 degrees azimuthal, -12 degrees elevation away from broadside, and that assigned to sub 2 to be 46 deg. az and 30 deg. el, the phase shift at each element in sub 1 must be:

$$\beta = (2 * \pi)/(\lambda) * (\lambda/2) * [i * sin(\theta) + j * sin(\phi)] \tag{4.2}$$

Where i and j are the element positions in each subarray in the azimuthal and elevation dimensions, and theta and phi are the steering angles in those directions.

For the scenario described, this becomes simply,

$$\beta = \pi * [(i-1) * sin(\theta) + (j-1) * sin(\phi)] \tag{4.3}$$

Where beta is measured in radians. A Chebyshev taper with 30 dB SLL is used, therefore the "map" of amplitudes and phases required at each antenna are shown in Figure 4.17:

A single bus of the "4-Bus" feeding network would appear as shown in Figure 4.18.

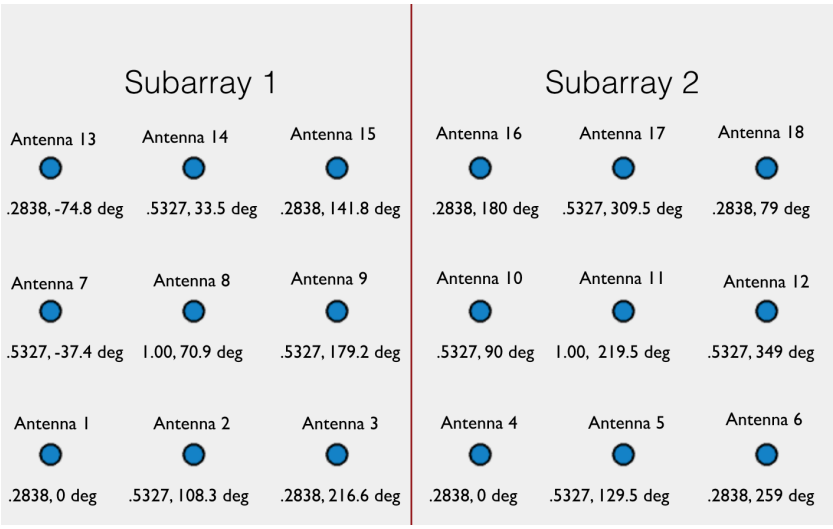

Fig. 4.17. Map of amplitudes and phases for specified array scenario

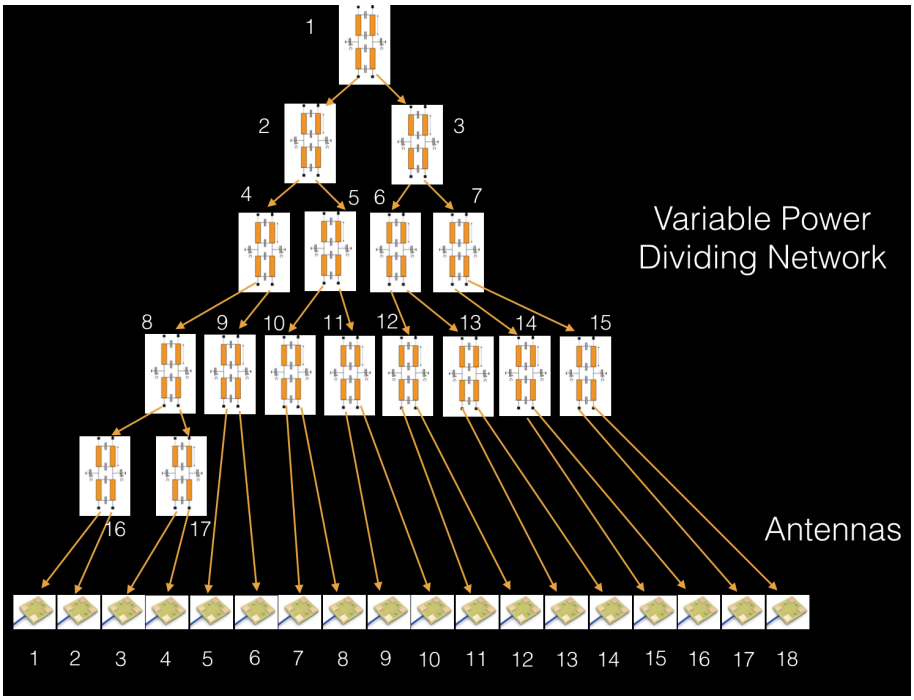

Fig. 4.18. Network of VPDs for each bus feeding specified array

The maximum dividing ratio achievable with the VPD being considered here is 100:1, and the minimum is 1:50 (where the ratio is written as Port 1:Port 2). The table in Figure 4.19 summarizes (for power Bus 0) the powers incident on each antenna due to this limitation (no infinite diving ratio).

Antenna	Power Required (from Bus 0)	Actual Power
1	0.2838	0.2782
2	0	0.0028
3	0	0.0028
4	0.2838	0.2782
5	0	0.0025
6	0	0.0025
7	0.327	0.3238
8	0.423	0.4188
9	0	0.0037
10	0	0.0037
11	0	0.0052
12	0.523	0.5178
13	0.519	0.519
14	0.074	0.074
15	0	0.00027
16	0	0.00027
17	0.3389	0.3389
18	0.054	0.054

Fig. 4.19. Table for Bus 0 showing errors resulting from lack of bypass node

When considering the error arising from this, it is found to be small: Both magnitude and phase errors are within 2 percent, at least for this particular scenario, and can be found in Figure 4.20. Exactly the result this would have on array performance isn't the primary consideration, although some resources are published on the broad topic [37]. This 2 percent seems to be reasonable margin of error–however, it cannot be guaranteed that these errors would not increase in some other scenario.

The addition of the envisioned bypass junction would reduce the error in this particular example problem, as shown in Figure 4.21, but not bring it to zero.

As can be rapidly understood, the error drops to zero for all but a very few cases, but some applications may suffer more from this issue, and some may require absolutely no error of this kind. Therefore, an additional modification is proposed. The reason for the remaining error is that, although infinite ratios are now achievable, there is a gap in between 100:1 and infinity which, although relatively infrequent, does sometimes occur, especially when parts of the array are in "dormant" or "listening mode", as was not the case here. An

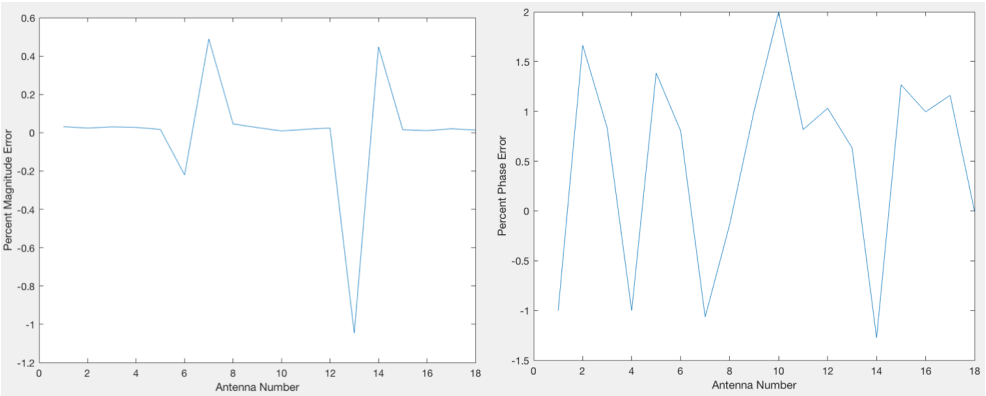

Fig. 4.20. Percent Phase and Magnitude Errors for 4-Bus Method without Bypass Junction

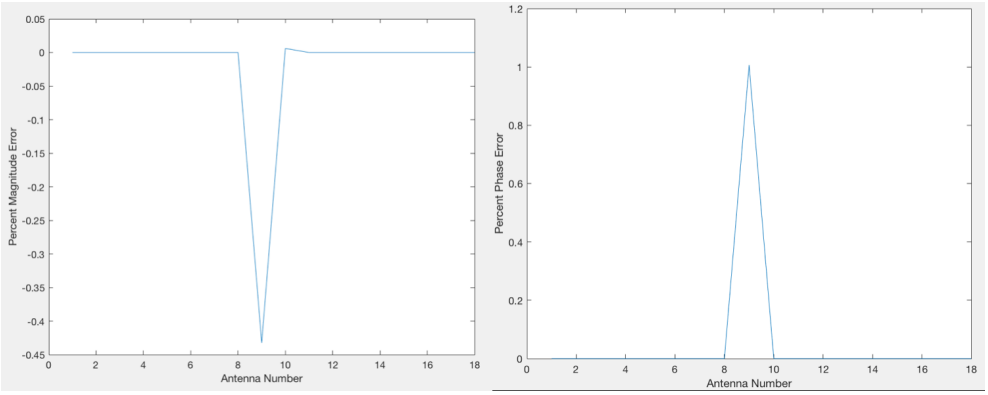

Fig. 4.21. Percent Phase and Magnitude Errors after addition of Bypass Junction

additional modification can be made to the system which would almost entirely remove the error. This is a fourth "path" down which the power can travel at each node, which takes it to a small "delocalized" group of variable power dividers. By having two variable power dividers in series (with clever use of a power combiner), dividing ratios can be achieved up to the square of that available with a single unit (see in Figure 4.22). These "delocalized" dividers allow devices which are not "pre-allocated" to any specific node to assist it if necessary.

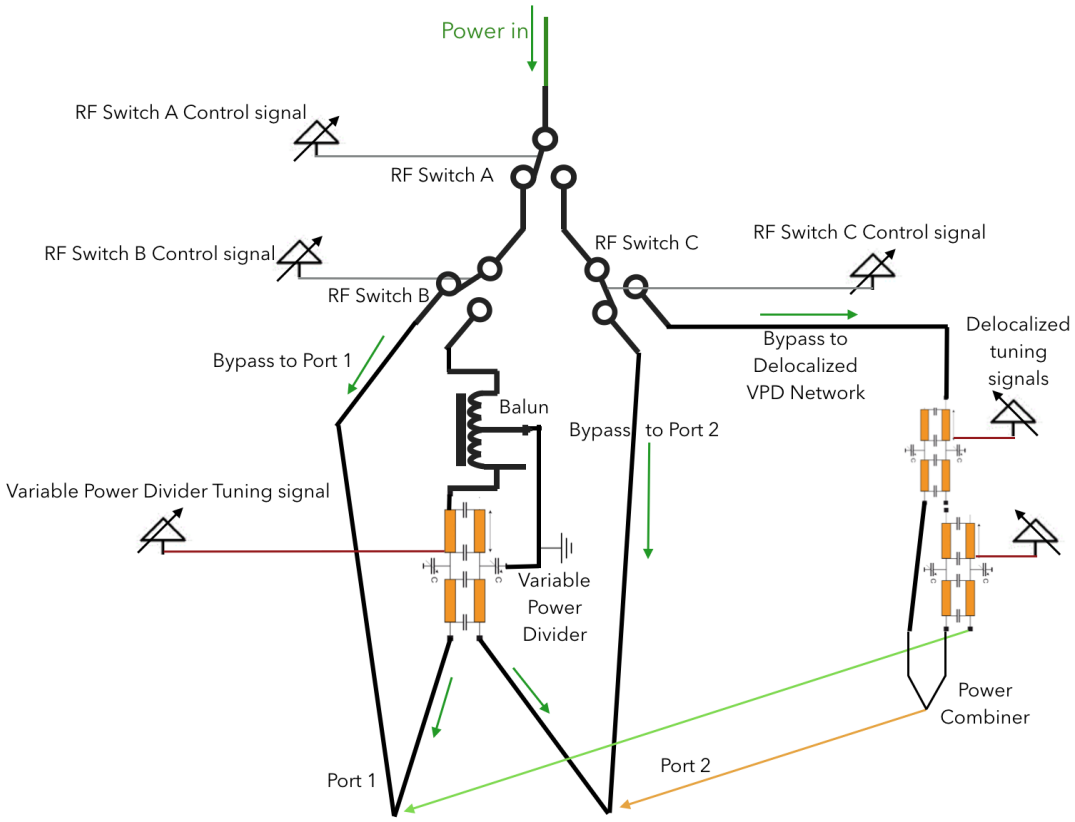

Fig. 4.22. “Delocalized” variable power dividers solve limitation of dividing ratio

It should be easy to see that this idea works, conceptually, but the real question is “How many additional VPDs do you need,and how will this affect the system cost?” Some simulations (results in Figures 4.23 and 4.24) have been run to answer this question, this time on a 20x20 rectangular array which always uses at least two of its columns for location positioning of receivers.

The number of additional VPDs which should be included in the system is the choice of the system architect, and would depend on the nature of the application. In a military application, where flawless performance near 100 percent of the time is crucial, this system would require about 60 percent as many delocalized power dividers as localized VPDs.

On the other hand, since most applications do not require such stringent measures, it may be acceptable to reduce the number greatly, and simply accept the slight, occasional loss in performance which will accompany the decision.

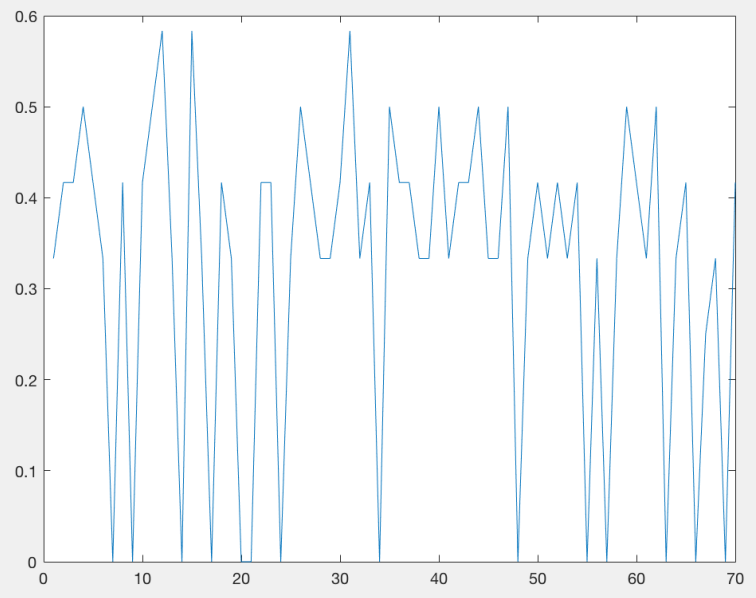

Fig. 4.23. Ratio of required Delocalized VPDs to localized VPDs over 70 random simulations

Additional VPDs (as % of localized VPDs)	Frequency of Error Free Operation
0%	20%
35%	57%
42%	81%
50%	96.5%
60%	100%

Fig. 4.24. Data Analysis on Delocalized Power Dividers

Cost of 4-Bus Method

The goal of the 4-bus method was to decrease the cost of phased array systems so that they could be used in many applications where expense was previously prohibitive, as well as create greater value in already existing applications. When an example bill of materials

is examined in comparison with classical systems and more modern, existing technologies, the results are striking (See Figures 4.25, 4.26, 4.27). This can be repeated with similar results for a system of any reasonably large size.

CLASSICAL			
	Count	Cost ($)	Manufacturer / Part
Amplifiers	8000	6.85	Minicircuits CMA-545
Phase Shifters	8000	39.77	Macom MAPS-010164-TR0500
Power Dividers	4095	1.05	Minicircuits BP2U
Control Signals	16000	0.07	
Heat Sinks	8000	0.10	
Total		~$379,170	

Fig. 4.25. Pricing of classical feed architecture (8000 element array)

The method proposed by Daniel Ehyaie in [10] is difficult to put into a study like this because of the vagueness of the specifications required for the separate “amplifier” and “variable gain amplifier”, but nevertheless, an attempt has been made. It is worth noting again, however, that the “Ehyaie Method” cannot achieve the same performance, in terms of magnitude of phase shift, as is possible with the “classical” or “4-Bus” methods.

Performing such a comparison as this is quite difficult, because “price points” is more a study of economics and negotiation than of engineering. Therefore, the author readily admits that many of these prices may not be the lowest that could actually be attained if a company attempted to purchase a quantity in the millions at once. The following are the assumptions used in order to attain these estimates:

1. For parts which are required in large quantities for each system, the price point listed is the lowest price point (highest quantity order) that could be readily discovered in online listings.

2. For the row in the table “Control Signals”, the cost is listed at 7 cents each based on the cost of standard microcontroller chips which may have 100 or more “IO lines”

3. Heat sinks cost is based on approximate cost of machined metal, and, being so small relative to other parts of the system, is not critical. The heat sink numbers match in the classical and “4-Bus” architectures because, although the amplifiers for the 4-Bus system have heat sinks included, it may be necessary to include heat sinks on the power combiners. This is because the signal summation results in constructive interference and power loss.

4. The cost of a variable power divider cannot be precisely predicted, because they are not widely available “off-the-shelf” at present. However, the divider presented in [29] is made up primarily of a pair of directional couplers, and another pair of hyperabrupt varactor diodes. Examining the bulk price points of these parts (including a built-in Balun), they are found to come (in total) to well less than a dollar. In the interest of leaning “on the safe side” of overestimating cost, the price point is placed at just over a dollar, equal in price to the “Constant (Wilkinson) Power Dividers”. Additionally, the cost of the baluns is assumed included with the VPDs.

5. The amplifier sizes were selected based on an 8000 element array where the maximum amplitude excitation for each antenna is 100 milliWatts.

It must be noted that the 4-Bus cost does not include signal processing circuitry, or the additional RF switch that is required with it. This additional cost is very dependent on which methodology is used, and is probably negligible regardless. Not only this, but by including this in our cost analysis, the 4-Bus method is no longer on “even ground” with the classical method, and therefore the comparison in terms of cost is not accurate; That is, if we really desire an “apples-to-apples” comparison between methods, we should leave out the cost of the receiving circuitry, because it is optional, and adds functionality which is neither available in the classical system, nor necessary in all applications.

EHYAIE			
	Count	Cost ($)	Manufacturer/ Part
Amplifiers	8000	6.85	Minicircuits CMA-545
Var Gain Amp	8000	10.71	Analog Dev 0.5 dB LSB GaAs MMIC 6-Bit Digital Variable Gain Amplifier SMT, 0.07 - 4 GHz
Phase Shifters	2000	39.77	Macom MAPS-010164-TR0500
Power Dividers	4095	1.05	Minicircuits BP2U
Power Combiners	400	1.05	Minicircuits BP2U
Heat Sinks	8000	0.10	
Control Signals	8001	0.07	
Total		~$226,100	

Fig. 4.26. Pricing of Ehyaie feed architecture (8000 element array)

4-BUS			
	Count	Cost	Manufacturer/ Part
Amplifiers	4	3,595	Minicircuits ZHL-100W-352
Phase Shifters	3	39.77	Macom MAPS-010164-TR0500
Constant Power Dividers	3	1.05	Minicircuits BP2U
Power Combiners	8000	1.05	Minicircuits BP2U
Local VPDs	4095	1.05	
Delocalized VPDs	2050	1.05	
Control Signals	18434	0.07	
Heat Sinks	8000	0.10	
RF Switches	12285	0.07675	Infineon BGS12SN6E6327XTSA1
Total		~$32,388	

Fig. 4.27. Pricing of 4-Bus feeding architecture (8000 element array)

Other Considerations

One “intangible” that should be considered is the effect of the reconfigurable nature of the system, particularly the “single control voltage bypass junction” on spatially fitting the transmission lines. It is clear that some of these complexities will require a “third dimension”; Some of these lines must cross over each other, in order to wind back and forth to the “delocalized variable power dividers.” It was also briefly investigated whether the lines crossing over each other would have an adverse effect on performance. [19] and [30] discuss how “mitered bends” in transmission lines, where the width of the line is carefully reduced around the bending section, allow the characteristic impedance to be kept constant, and minimizes losses due to reflection. Indeed [19] states that mitering properly reduces the added capacitance due to the bend, “restoring the line back to it’s original characteristic impedance.” Therefore, there is no reason to believe that one line going “up and over” the other would cause problems. If both are properly shielded and all proper care is taken, should greatly degrade performance. Indeed, formulas are presented in order to handle mitering properly. The dimensions described in these formulas can be visualized in Figure 4.28 [19].

$$D = W * \sqrt{2} \tag{4.4}$$

$$W * \sqrt{2} * (0.52 + 0.65 * e^{-1.35 * W/h}) \tag{4.5}$$

$$A = X * \sqrt{2} - W \tag{4.6}$$

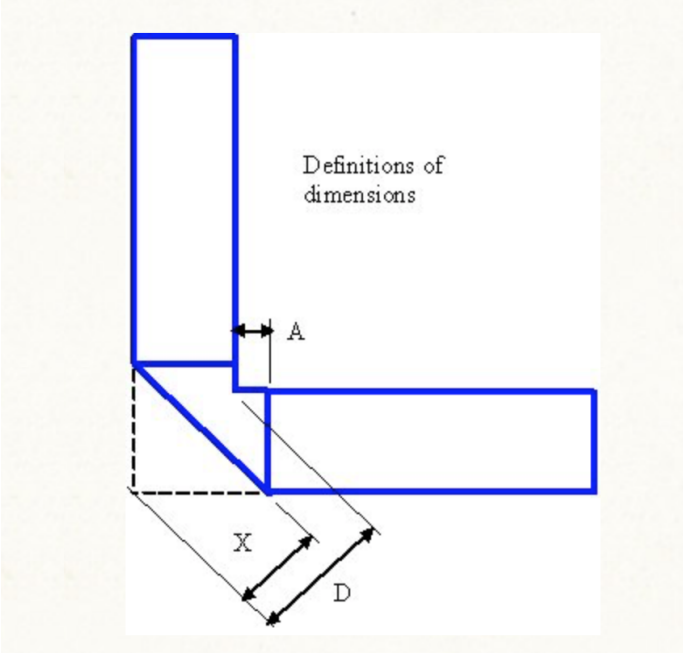

Fig. 4.28. An example of how “bend mitering” is used to maintain constant impedance [30]

4.5 Additional Discussion

This reconfigurable array solves multiple issues with existing solutions. System flexibility is vital for all dynamically changing, unpredictable systems: Flexibility of both amplitude and phase shift is traditionally obtained by having a discrete phase shifter and amplifier for each antenna, but the cost of this can be exorbitant. Not only is it unnecessary and expensive to have these large counts of separate discrete components, but, in an array such as this, where the required amplitude and shift levels must constantly change, a classic system design forces the system architect to purchase large quantities of “wasted” resources. That is, for a (reconfigurable) system where the maximum taper per antenna 1 watt, each antenna must be supplied with an amplifier capable of 1 watt, because the dynamic nature of the system means that any antenna might find itself in the maximum taper

position for some configuration. It is only a small percentage of the time, however, that many of these actually find themselves it that position. Therefore, the system possesses large quantities of unused resources.

With this reconfigurable array, the system architect can calculate or simulate various configurations of the system and find the maximum possible **total** instantaneous power burden of each amplifier, choose just a bit more capacity then that, and greatly decrease her or his cost. In fact, it is shown in the next section that the total purchased capacity for the proposed system need be only about **one half** of that required in "classical methods".

As compared to the "Ehyaie Method", the "4-Bus Method" makes it possible to achieve phase shifter count reduction in planar arrays–that is,the use of vector summation to achieve phase shifts. Ehyaie's method operated in a linear feed, and therefore, was only feasible for linear arrays. For two-dimensional arrays which use a corporate feed, however, the "4-Bus Method" is not only feasibly, but can achieve any inter-element phase shift–whereas Ehyaie was very limited. Corporate and series feed architectures are shown in Figure 4.29.

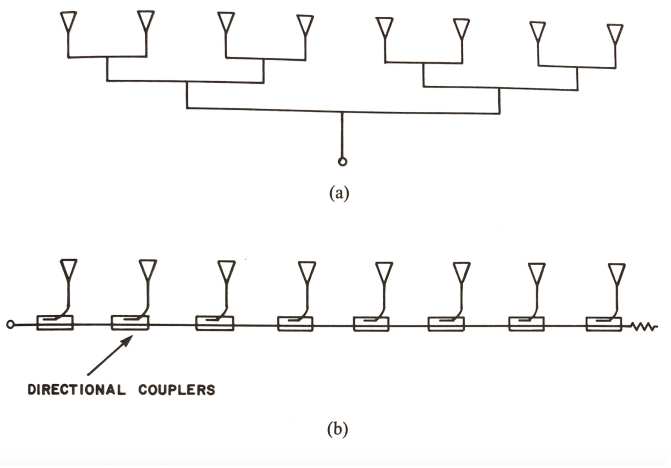

Fig. 4.29. (a) Corporate Feed Network (b) Linear Feed Network [11]

Additionally, from an array perspective, its dynamic nature allows improvement over current technology for applications such as drone defense. With slight (linear) reduction in performance, the array can transmit to an increased number of targets, decreasing the size

of each subarray. Although there exist some systems (primarily defense related) which can rapidly switch between targets, the author knows of no existing systems for wireless power transfer which can simultaneous transfer to a large, dynamic number of targets.

The "bypass node" which was implemented to enhance the feeding architecture could itself be a useful tool in many other applications. In conjunction with a variable power divider, it allowed all the power to be passed to one port or the other, to be "diverted" toward delocalized VPDs, or to enter the primary VPD, all without requiring an additional control voltage (for the bypass node at least–the delocalized VPDs require separate control) besides the one that would be needed to tune the VPD regardless.

Finally, it is worth noting that this feeding architecture is not limited only to reconfigurable arrays or to arrays for wireless power transfer, but could help reduce the cost of phased arrays in many industries and applications.

4.6 Applications

In the author's perspective, there are four primary types of applications which should be considered for this technology:

1. Military High Power / Space Solar Power

High power applications either to transmit intense beams of power for capturing some distance away, or for a defense application, such as destroying a hostile drone.

2. Millitary Low-Medium Power

There are Radar phased arrays which could benefit from the reconfigurable nature of the system, and particularly from the low cost "4-Bus" Feeding Architecture.

3. Commercial Charging

Automated Guided Vehicles (AGVs), drones, cell phones are just a few of the many applications for technology such as this. One of the visionary applications for this work was to charge a "Mobile Robot" (a type of AGV) from a Material Handling "Goods to Person" system such as "AutoStore" (see Figure 4.30). These systems must contain twice as many robots as they actually need, because the devices spend about 50 percent of their

lifetimes charging. These robots are so expensive that a “Ceiling Mounted” reconfigurable array which powers all of the robots during operation could dramatically reduce the system cost by reducing the “excess robot count” required. Given the current state of Governmental Regulations about high power radiated emissions, a system like this would almost certainly need to be in an extremely isolated chamber, shielded from humans, for safety and interference reasons.

Fig. 4.30. A mobile robot from an “AutoStore Goods to Person” system [51]

4. Low Power (Communications Application)

Anything goes here. The reconfigurability and inexpensive feeding architecture will reduce the cost of many arrays for dynamic applications and make them affordable in industries where they were previously excluded.

5. AUTHOR'S CONTRIBUTION: PHASED ARRAY RESULTS

In order to maximize performance and make appropriate selections for each application, it's important to understand both qualitatively and quantitatively the performance of arrays of various geometries and element spacings for various situations. It's fair to say that the studies performed here, including thousands upon thousands of simulations, were utterly extensive, and results were both useful and, in some cases, surprising.

5.1 Square (Rectangular) Arrays

Square arrays with spacing from half a wavelength up to a wavelength were considered. Alternatives below a half wavelength yield inferior gain characteristics with no real benefits, and increasing to above one wavelength will no longer improve the gain, while worsening sidelobe performance. Traditional array theory states that the array gain will decrease with the cosine of the steering angles, both in azimuthal and elevation directions [35]. This was found to hold exactly as expected for arrays with 0.5 lambda spacing, as shown in figure 5.1. The figure shown can be explained as follows: The azimuthal angle would be held constant, while the elevation angle was varied from 0 degrees up to 60 degrees. The beam directivity would be recorded for each simulation. Once the elevation angle reached 60 degrees, the azimuthal angle would be changed to higher value, and this process was repeated until the azimtuhal surpassed 60. All of this was for a 39 x 39 array with constant tapering.

When the element spacing is increased to .65 lambda (see Figure 5.2), however, some rather unexpected results are found. Peak directivity no longer decreases directly with the cosine of the steering angles. It is notable that, at the low values of azimuthal steering,

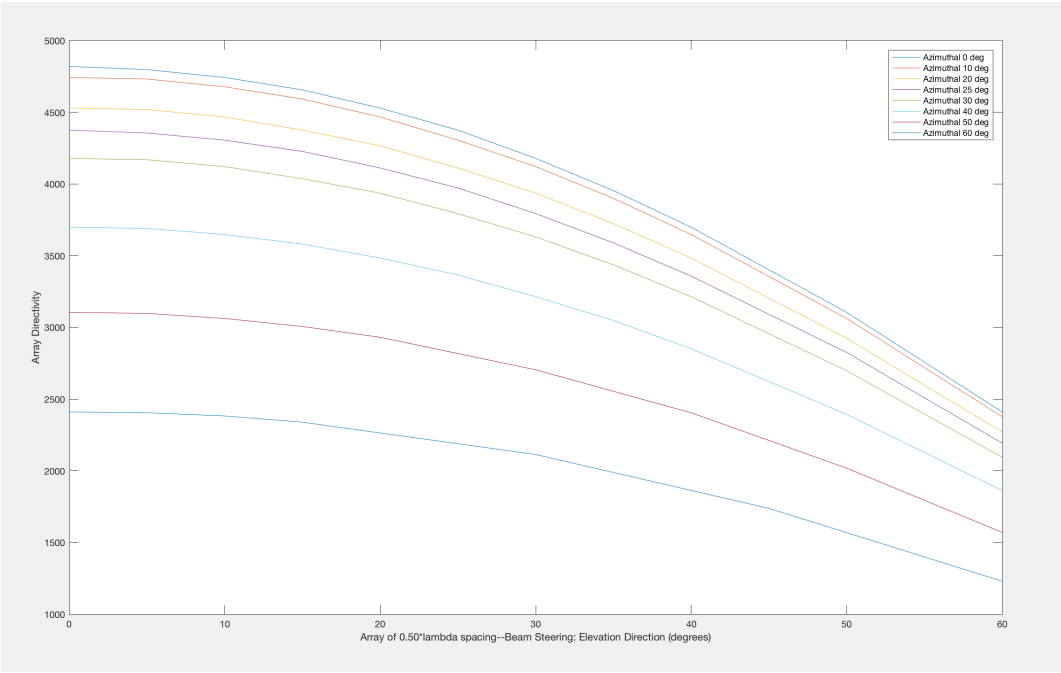

Fig. 5.1. Square 39x39 array with 0.50 Lambda Spacing–Perfectly matching expected results

the results proceed similarly to those expected. Only once the azimuthal angle becomes large does this "hump" appear, and it appears at a larger elevation angle for large azimuthal angles.

It is difficult without extensive analysis into the physics of coupling between elements to explain precisely the reason, but it has been determined that is related to the size of the grating lobes for each case. The steering angles of 40 degrees azimuthal, 10 deg. elevation, and 40 deg. azimuthal, 20 deg. elevation are now examined in order to demonstrate this.

The directivity is found at the point 40,10 (40 deg. az, 10 deg. el) to be 36.12 dBi, while at 40,20, it comes to 37.06 dBi. A comparison of 3-D radiation patterns (Figure 5.3) reveals the reason: The larger grating lobe (approximately 29 dBi, compared to 23.5 dBi) is found at the smaller steering angle! This "leakage" of power brings the overall gain for the main lobe down. Explaining and predicting the grating lobe phenomena is beyond the scope of this thesis, but the "trickle-down" effect that these lobes have on wireless power transfer is well worth noting, while the effect itself is worthy of further study in the future.

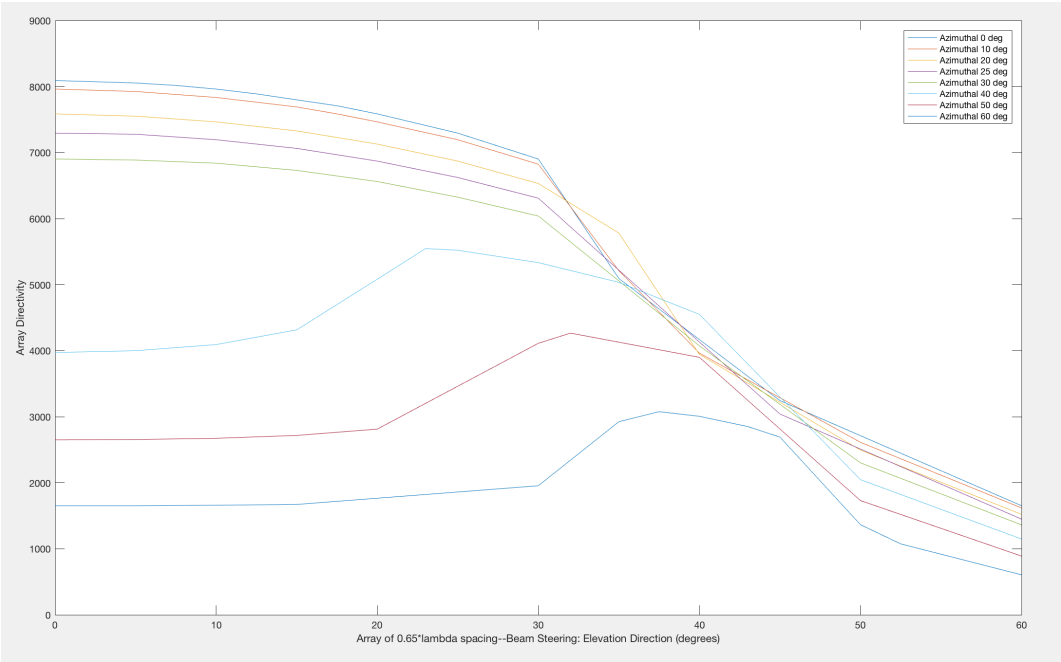

Fig. 5.2. 39x39 Rectangular Array with 0.65 Lambda Spacing

By examining the additional results which follow, it is clear that they are dependent on the inter-element coupling which is effected by both spacing (relative to wavelength) and beam steering angles.

For brevity's sake, the full plots for spacings of .68, .70, .80, and .90 lambda are not included here, but can be found for reference in the appendix. Included here, however, are the results for .75 lambda (Figure 5.4), .98 lambda (Figure 5.5), and 1 lambda (Figure 5.6).

The results are by no means identical, but follow a similar pattern to that of the previous study. One notable difference is that the "peak directivity" in each case is greater for the .75 spaced array, as the .65 array was greater than the .50 array. Picking up on this pattern, studies were also conducted for .98 and 1 lambda spacings.

As the results of .98 and 1 lambda spacings are considered, it is remarkable to note that, the highest directivity found in any simulation out of hundreds upon hundreds, is at the steering point 0,0 for .98 lambda. This result is noticeably higher than the corresponding one for the 1 lambda array, but, since this one point is not necessarily representative of the whole, the study cannot end there.

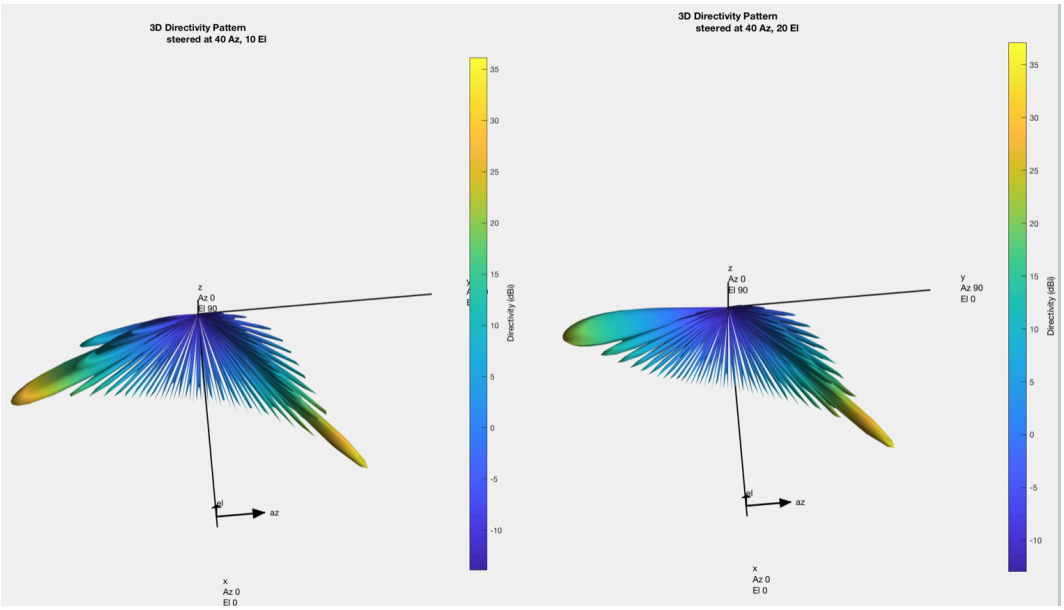

Fig. 5.3. Smaller beam steering angle (left) can actually result in larger grating lobes, reducing gain, for some element spacings above half lambda

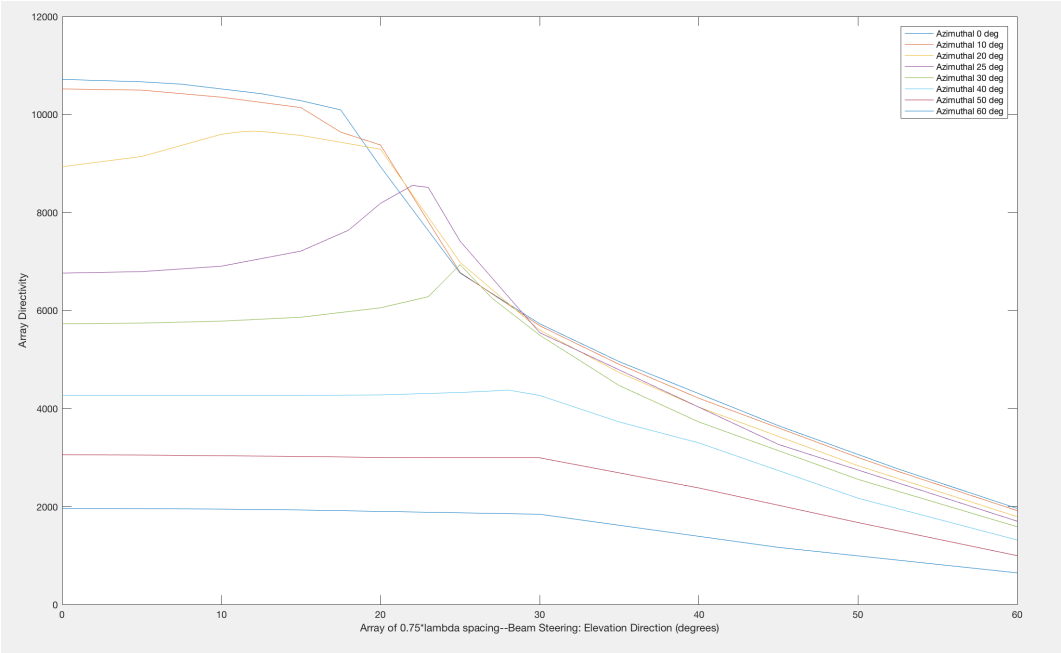

Fig. 5.4. Array with .75 lambda spacing–Results similar to .65 lambda

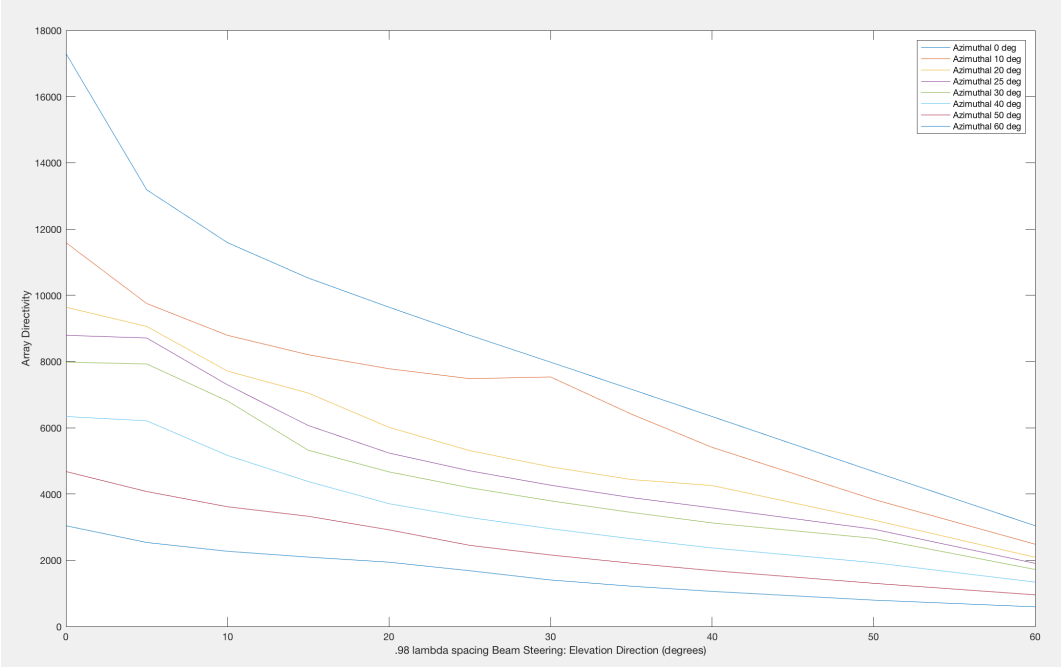

Fig. 5.5. Array with .98 lambda spacing

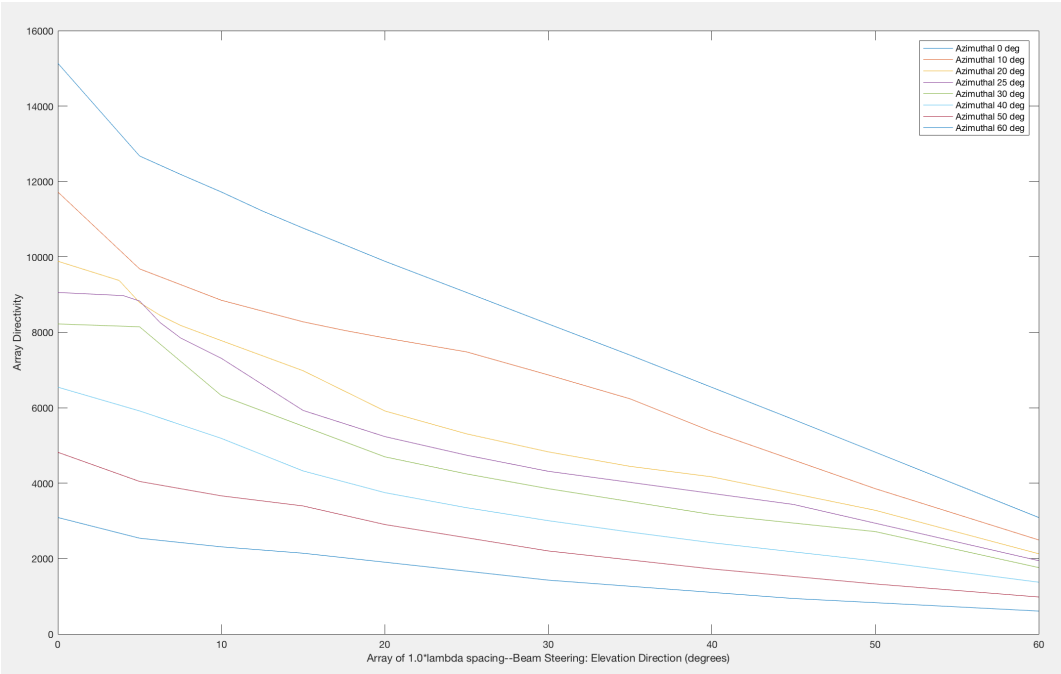

Fig. 5.6. Array with 1 lambda spacing

It would be interesting to see a "superposition" of all the spacings, at least for a single azimuthal value, held constant. It's shown in Figure 5.7.

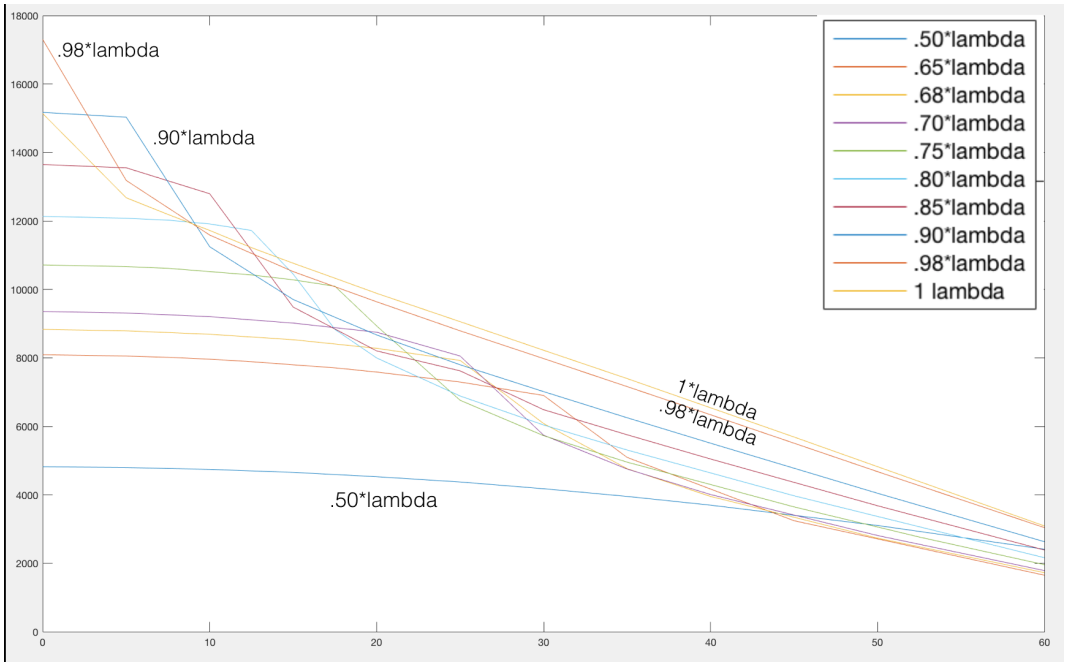

Fig. 5.7. At azimuthal steering angle of 0 degrees, comparison of many spacings

In the light of this, it is obvious that the .98 and 1 lambda choices are indeed the best, if the only goal is to maximize power transfer efficiency. To compare the two across the entire spectrum (from 0 to 60 in both azimuthal and elevation), a 3-dimensional fit must be performed for each. The fits were (understandably) very similar, and the one for 1 lambda is pictured below. In order to obtain the desired values, a complex calculation must be performed (shown in Figure 5.8):

$$AverageGain_{allangles} = [1/(60*60)] * \int_0^{60} \int_0^{60} G(\theta,\phi) d\theta d\phi \tag{5.1}$$

For the 1 lambda array, this comes to:

$$[1/3600] * (\int_0^{60} (\int_0^{60} 13970 - \theta * 219 - \phi * 234 + \theta^2 * .701 + \phi * \theta * 2.232 + \phi^2 * 1.033 d\theta) d\phi) \tag{5.2}$$

Which is 4,469.60. The equivalent calculation for .98 lambda yields 4,459.72. Therefore, although the .98 lambda array has the highest directivity of any considered for the 0,0 steering angle, the average across all angles is larger for the 1 lambda array. Because all spacings in excess of 1 lambda have degraded performance, the conclusion is safely reached that **the choice of 1-lambda spacing will result in the highest peak directivity and power transfer efficiency when averaged across all steering angles for square arrays**.

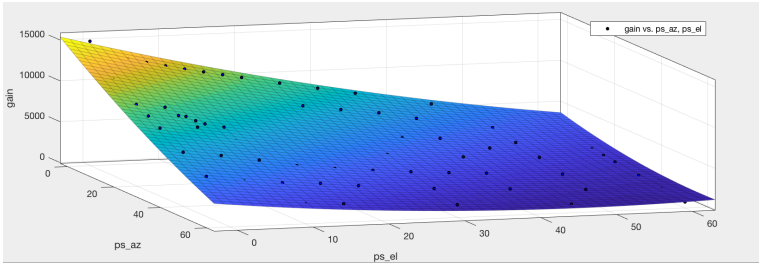

Fig. 5.8. Quadratic fit for 1 lambda rectangular array as function of elevation and azimuthal steering angles

Furthermore, it would be extremely useful if we could obtain, for a square array of 1 lambda spacing, a relatively good approximation of directivity (gain) as a function of theta, phi, and the number of elements. An approximation such as this would save massive amounts of time in "early stage project planning". Instead of having to run many complex calculations to get initial estimates for directivity, wireless power efficiency, etc., the results could be closely estimated with this single formula. We have the gain as a function of theta and phi, for a fixed size (39x39) of array. Comparing this point by point to an array of 25x25 yields Figure 5.9. Similar results were obtained for comparisons to 20x20 array. Realizing that the ratio between the number of elements is 1521/625, which comes to 2.43, there is small enough divergence at the various steering angles that it seems a reasonable approximation to treat the gain as directly proportion to the number of elements in the array, for any steering angle. This is the equation that is obtained from a fit combined with the linear assumption just stated.

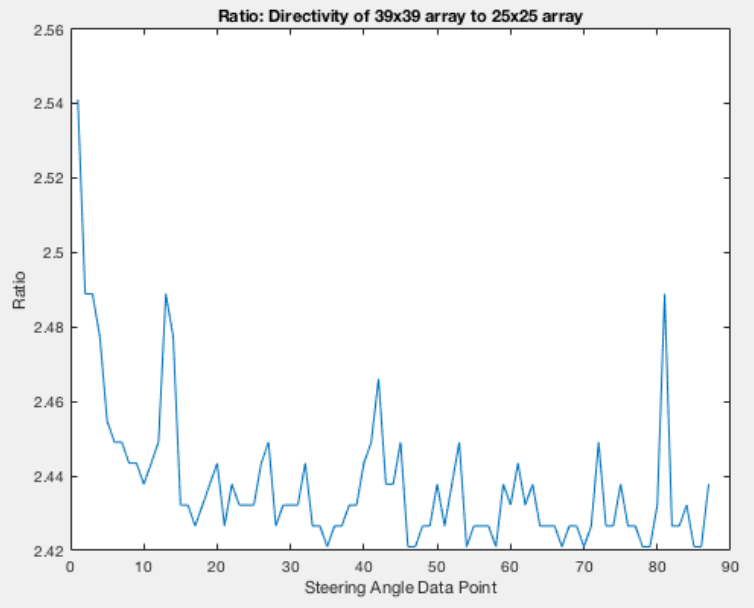

Fig. 5.9. Ratio of Gains in 39x39 Rect Array and 25x25 Array for corresponding beam steering points

$$Gain(\theta,\phi)_{rect1} = (numelements/625)*(5643-86.4\theta-92.69\phi+.2515\theta^2+.8869\theta\phi+.3892\phi^2) \tag{5.3}$$

Checking this for validity, we examine several different size arrays at various angles (see Figure 5.10), and find that is not nearly accurate enough.

However, the peak gain may be able to be linearized:

$$Gain_{PeakRectArray1lambda} = -390.7 + 10.2 * numelements \tag{5.4}$$

Checking these results, we see in Figure 5.11 that for arrays of 400 elements or more, the simple function has excellent performance, and could save engineers setting out on a project like this from having to perform extensive simulations right away.

#Elements	Azimuthal	Elevation	Measured Gain	Calculated Gain	% Error
484	30	30	1233.1	1274	3.2
484	10	40	1710.01	1606.13	6.07
784	20	30	2500.35	2655.97	6.22
900	30	5	4797.33	4257.6	11.25

Fig. 5.10. Poor results show that fit has utility only for rough approximations

#Elements	Measured Peak Gain	Calculated Peak Gain	% Error
256	2317.4	2220.5	-4.18%
324	2,971.66	2914.1	-1.94%
361	3,334.3	3,291.5	-1.28%
400	3,715.4	3689.3	-0.7%
576	5457.6	5484.5	0.49%
900	8729.71	8789.3	0.68%
1225	12078.14	12104.3	0.22%

Fig. 5.11. Excellent results are found for arrays with 400 or more elements

Because we have shown that not all array sizes are affected by beam steering at the same rate of attenuation, the one study that remains to perform would be a fit of the "average gain" across all beam steering angles of interest. The function fit is considered at several points (see Figure 5.12), and, at least in initial considerations, appears excellent.

$$Gain_{Averagedover\theta,\phi} = 4.361 + 2.936 * numelements \tag{5.5}$$

#Elements	Measured Average Gain	Calculated Average Gain	% Error
400	1,179.92	1,178.76	0.098%
625	1,837.35	1,839.36	0.109%
1521	4,469.6	4,470.02	0.0094%

Fig. 5.12. Average Gain Fit Demonstrates Excellent Results

The "measured values" were obtained by performing a function fit on nearly 100 data points of various beam steering angles, then integrating (as was demonstrated earlier in this chapter) across the region of interest and normalizing. For example, this is the calculation that was performed for the array of 20x20:

$$[1/3600]*(\int_0^{60}(\int_0^{60} 3572-\theta*52.95-\phi*58.07+\theta^2*.132+\phi*\theta*.5544+\phi^2*.2343d\theta)d\phi) \tag{5.6}$$

5.2 Tapering with Rectangular Arrays

It is worth considering the effect of tapering on the results. Chebyshev tapering is frequently employed for sidelobe level reduction, but has the negative effect of decreasing the peak directivity. There are certainly applications in which tapering is extremely useful, but a brief analysis has demonstrated that, although wonderful for sidelobe reduction, tapering does not alleviate the issue of grating lobes (see Figure 5.13). That is, for arrays with grating lobes, tapering simply reduces peak directivity without solving the biggest issue of all. For this reason, further studies will consider tapering only for arrays with sufficiently small element spacing (close to .50 lambda) [52] to eliminate all grating lobes.

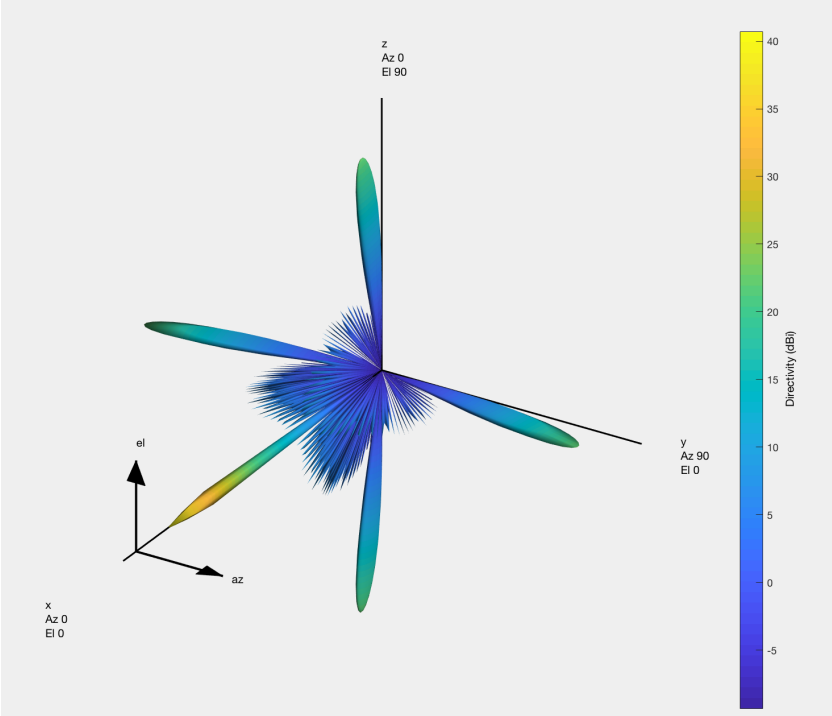

Fig. 5.13. Chebyshev tapered rectangular array has reduced sidelobe level, but still large grating lobes

5.3 Hexagonal Arrays

The hexagonal array with .8 lambda spacing presented by [1] resulted in an enormous gain with very low sidelobe levels. The large inter-element spacing, however, leaves the system extremely vulnerable to grating lobes. It would be useful to examine the performance of this array versus an equally sized array with .5 lambda spacing, to gain at least a qualitative understanding of their characteristics.

The comparison was performed at six points with greatly varying steering angles. A close inspection of the data shows that the .8 lambda spacing generally, but not always, yields superior gain. The sidelobe level tends to be higher for the .8 lambda array, but there is no consistent pattern in regard to sidelobe reduction from the peak gain. The most important factor, however, is the grating lobes. For all considered steering angles except perfectly

broadside, the array with .8 lambda spacing had large grating lobes, approximately as large as the main beam itself, whereas the .5 lambda array has, by definition, no grating lobes at all [52].

It is clear from this, therefore, that .5 lambda spacing should be chosen for applications where low sidelobes (and no grating lobes) is critical (Figures 5.14 and 5.15).

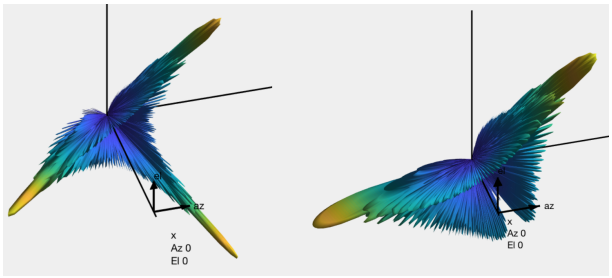

Fig. 5.14. Example of grating lobes from a hexagonal arrays of 0.65*lambda (right) and .80*lambda (left) spacing

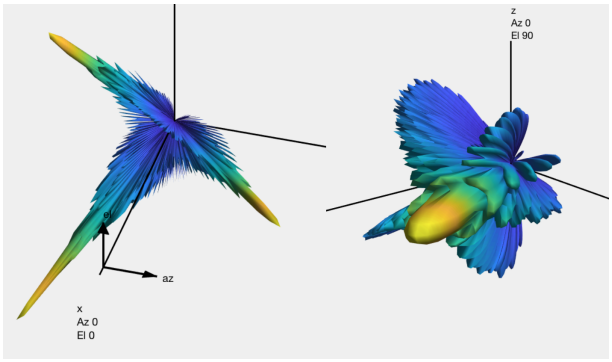

Fig. 5.15. With beam steered to 40, 10, patterns from hexagonal arrays of 0.50*lambda (right, no grating lobes) and 1*lambda (left) spacing

What type of performance can be expected from a .5-lambda hexagonal array without tapering? This is investigated in the next section, relative to a square 1-lambda array with similar element counts.

5.4 Comparison of Hexagonal and Rectangular Arrays

It is intrinsically worthwhile to possess a comparison between hexagonal and rectangular geometries. SLL and directivity are shown in Figures 5.16 and 5.17 respectively, with it being understood that either will possess grating lobes if the element spacing is much in excess of half a wavelength [52]. This understanding takes us far–If grating lobes, which can be equal in magnitude to the main beam, exist, then no amount of sidelobe level reduction truly solves the problem at hand, whether related to safety or interference.

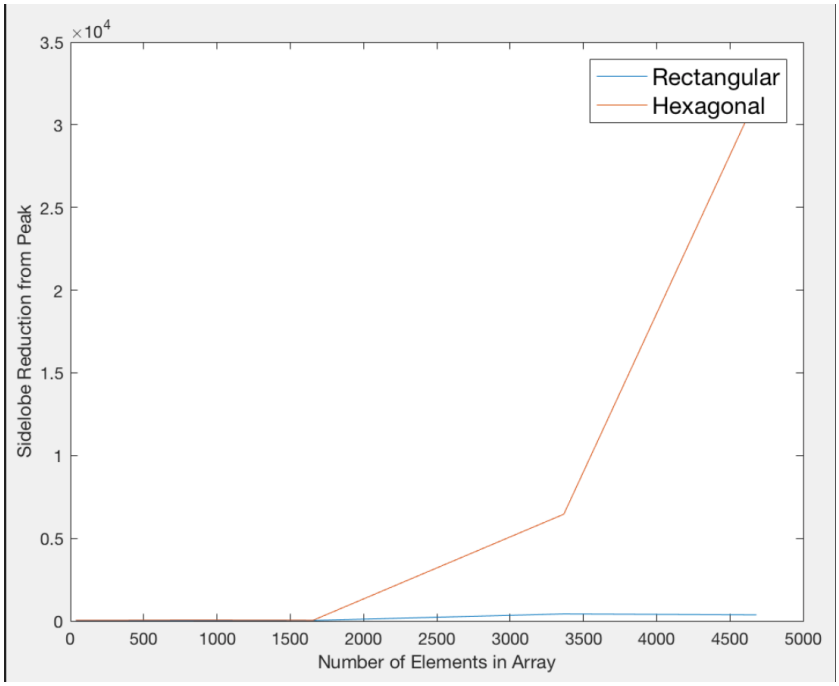

Fig. 5.16. Hexagons have significant advantage in sidelobe level

One way to consider this is in terms of the type of application the array is used for. If the goal is to maximize directivity, it is clear from Figure 5.17 that a rectangular array is the way to go. On the other hand, if the goal is eliminate side and grating lobes, a hexagonal array is clearly the best choice. When it comes to the question of what the element spacing should be within that hexagon however, the conclusion is quickly drawn that it must be near to half a wavelength in order eliminate grating lobes without sacrificing directivity needlessly (directivity goes down with no real side benefits when the spacing is

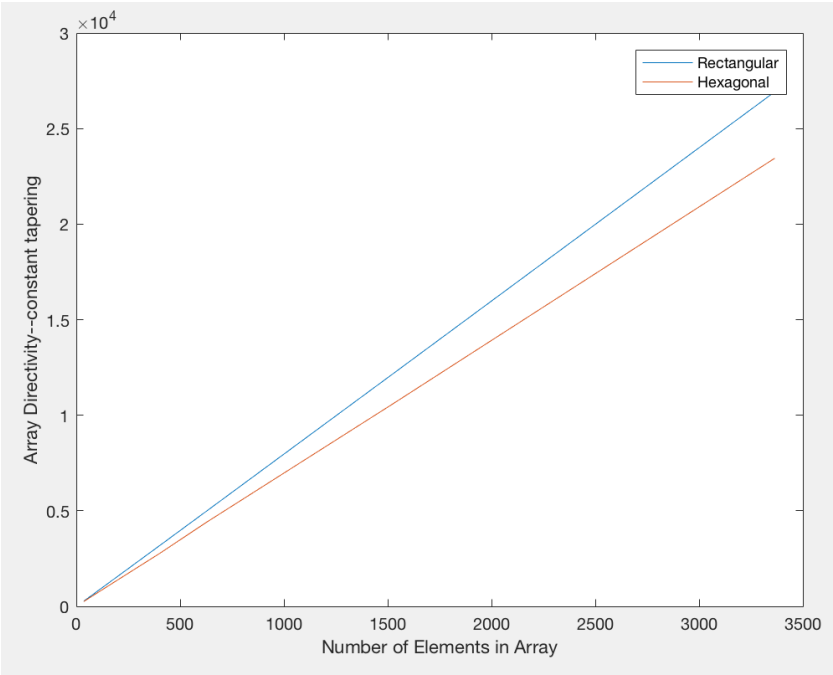

Fig. 5.17. Rectangular arrays have significant advantage in directivity

decreased below half lambda). That is, it would be pointless to use a hexagonal array (the merit of which is sidelobe reduction) if one is going to select a spacing which will produce uncontrollable grating lobes, anyways.

Rectangular Arrays with 1 lambda spacing are the best options if the goal is to maximize directivity and efficiency. Hexagonal Arrays with 0.5 lambda spacing are the best options if the goal is to eliminate sidelobes and grating lobes.

The primary contributions of this thesis were not focused on improving the achievable wireless power efficiency, but rather, on decreasing the cost of existing technology, and on understanding the strengths and weaknesses of those existing technologies. Nevertheless, it is worthwhile to conduct at least a quasi-quantitative analysis to observe the performance of existing technology when modified by the proposals within this thesis.

We know from [46] that the Space Transmission Efficiency, or "STE", denoted by τ, is proportional to the square root of the transmitter's effective aperture area.

$$\tau = \sqrt{A_T * A_R}/(\lambda * R) \tag{5.7}$$

Substituting the value for transmitter effect aperture area (and still assuming far-field):

$$\tau = \sqrt{(Gain_T * A_R)/(4 * \pi * R^2)} \tag{5.8}$$

Therefore, the STE is proportional to the square root of the transmitter gain (in linear terms), if the receiver effective aperture area and transmission distance are held constant. Considering this in regard to a square (rectangular) array with 1 lambda spacing, we can derive some approximations for the effect of the "subarray splitting" upon the power efficiency.

If the entire system must split into n subarrays, then each subarray will be 1 / nth the size of the original array. For this examination, we will neglect the technicality of wondering whether or not this would result in an integer number of elements in each subarray, and simply consider everything to be a continuous function.

Altering our previously tested "fit":

$$Gain_{persubarray} = -390.7 + 10.2 * (systemelements/numsubarrays) \tag{5.9}$$

Which should be a solid approximation as long as each subarray is a square of at least 400 total elements. Therefore, if the entire system is said to have 10,000 elements, we can plot the approximate, relative STE as the number of subarrays is increased; Of course, the maximum value will be found when there is only one "subarray"–the array itself.

Because we hold effective receiving aperture and transmission distance constant, we can take all calculations relative to a τ_0, which will be, in the scenario described:

$$\tau_0 = \sqrt{(101609.3 * A_R)/(4 * \pi * R^2)} \tag{5.10}$$

τ then becomes:

$$\tau = \tau_0 * \sqrt{((102000/numsubs) - 390.7)/101609.3} \tag{5.11}$$

Which can be viewed graphically in Figure 5.18.

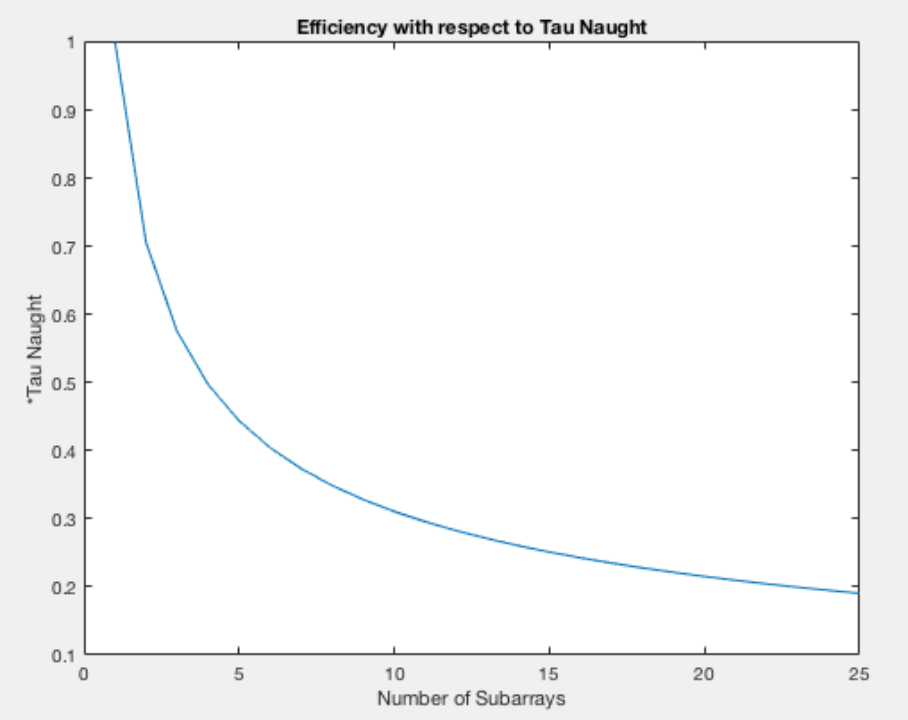

Fig. 5.18. Space Transmission Efficiency relative to τ_0 as array is separated into subarrays

We can compare the behavior of this square array system to a .5 lambda-spaced hexagonal one with similar number of elements. Because there will be a separate τ_0 for both the hexagonal and square arrays, it was decided to put the behavior of both arrays in terms of the τ_0 for square arrays, which will be called "Tau Max". This is shown in Figure 5.19.

Tau for the .5-lambda hexagonal array (entire system of 10,000 elements) can be quantified as well:

$$\tau_{0hex} = \sqrt{(27955.85 * A_R)/(4 * \pi * R^2)} \tag{5.12}$$

τ then becomes:

$$\tau_{hex} = \tau_{0hex} * \sqrt{.86 * ((28109/numsubs) - 153.15)/27955.85} \tag{5.13}$$

Note that this value for the hexagonal array requires additional approximation in order to account for the inability of hexagonal arrays to perfectly "split" into smaller hexagons– there must be some elements which are "left out", which is different for each size of sub-array, and, based on tests conducted at several array sizes, is estimated here as about 14 percent of the elements. The exactness of this number is not critical, however, as, regardless, the hexagonal array is shown to substantially lag behind the square array's achievable tau values.

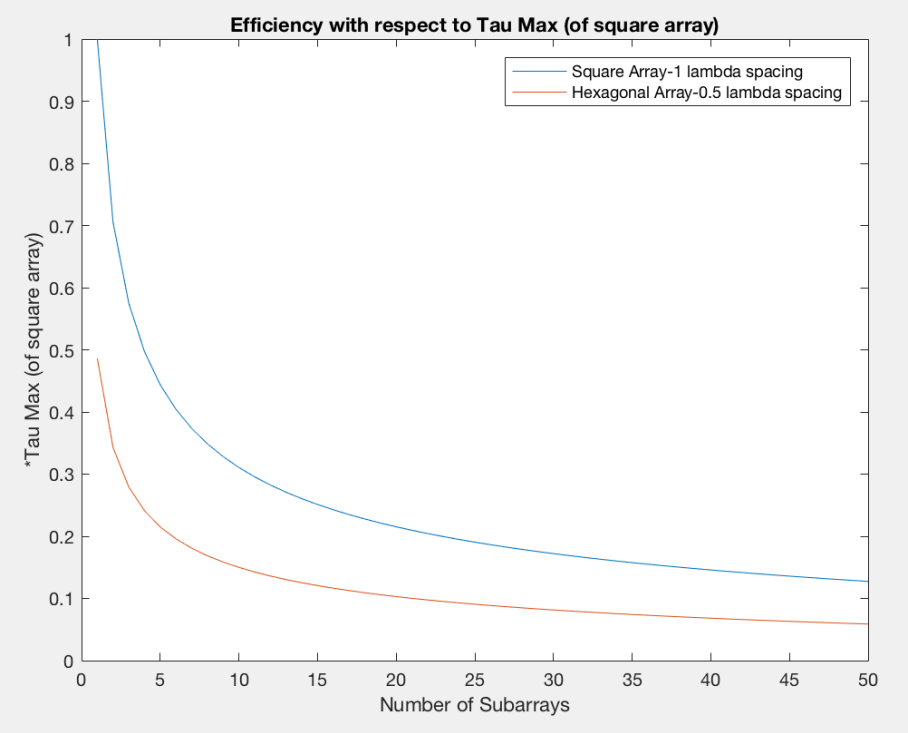

Fig. 5.19. Approximate Space Transmission Efficiency for .5-lambda hexagonal and 1-lambda square arrays of similar element counts, relative to an "undivided" square array

6. SUMMARY AND FUTURE WORK

In summary, this thesis has proposed a unique reconfigurable phased array which can simultaneously deliver power to a dynamic number of targets or receivers for many applications. The array was not limited to a single geometry, but rather, a multitude of geometry and element spacing combinations were considered in order to gain an understanding of how all relevant variables affect performance. Rectangular arrays were investigated and found to possess superior directivity but significantly worse sidelobe level when compared to hexagonal arrays. It was further found that, on average, across all relevant beam steering angles, these rectangular (or specifically, square) arrays maximized their directivity when the spacing between elements was exactly equal to one wavelength. Because of this, a 1 lambda spaced square array becomes a topic of great interest, and function fits and approximations were developed in order to allow quick calculations without even running simulations.

Additional studies were performed to understand hexagonal arrays, due to their superior sidelobe performance. Hexagonal arrays, like rectangular arrays, tend to possess grating lobes when the element spacing is much greater than half a wavelength. Because the presence of grating lobes is not necessarily eliminated by tapering, and rectangular arrays are known to possess superior directivity, this essentially eliminates hexagonal arrays with spacing much greater than .50 lambda from contention in any applications of interest. That is, hexagonal arrays of .50 lambda spacing are the best option for low side lobe, no grating lobe applications, while rectangular arrays with 1 lambda spacing and no tapering are the best option for applications which only seek to maximize power transfer efficiency. Nevertheless, some relative “Space Transmission Efficiency” comparisons were made to quantify the differences, and the effect of “reconfiguring” the arrays into many subarrays.

The reconfigurable array is made possible by a unique feeding architecture, which might hold the key to greatly reducing the cost of phased array technology in many applications worldwide. The feeding architecture, dubbed the "4-Bus Method", is treated extensively in the thesis, and, with perhaps the lone drawback of noticeable internal power losses, possesses many attractive features. A novel "bypass node" along with "delocalized variable power dividers" allows a system with N antennas to replace N amplifiers and N phase shifters with 3 phase shifters and 4 (potentially large) amplifiers. This improvement is further quantified by the newly-coined measurement "Resource Cost Effectiveness", or "RCE", which shows that, for some systems, the proposed feeding architecture requires substantially reduced total amplifier capacity compared to traditional methods.

Future work could focus on experimentation with exotic array geometries and "thinned arrays" in an attempt to continue increasing the maximum achievable directivity. Additionally, it would be worthwhile to continue researching the "variable power divider" to try to boost the possible dividing ratios, alleviating the need for the discussed "delocalized dividers". Relatively little is understood about rectenna technology–therefore, it would be valuable to study and invent new methodologies. Finally, if the safety aspect of WPT could be examined, and some method or operating frequency could be found such that the waves would not present a health hazard, this would go a long way toward advancing the technology.

REFERENCES

REFERENCES

[1] P. J. Schubert, "Sidelobe Reduction for GEO to Earth Wireless Power Transfer," *Proceedings of International Astronautical Congress*, 2016

[2] B. A. Kopp, M. Borkowski, G. Jerinic, "Transmit/Receive Modules," IEEE Transactions on *Microwave Theory and Techniques*, Vol. 50, No. 3, March 2002

[3] D. Parker, "Phased Arrays–Part I: Theory and Architectures," IEEE Transactions on *Microwave Theory and Techniques*, Vol. 50, No. 3, March 2002

[4] "LaserMotive", n.d. , [Online]. Available: https://en.wikipedia.org/wiki/LaserMotive [Accessed March 31, 2018]

[5] M. Nero, "Lasers In Pictures", n.d., [Online]. Available: http://www.laserfest.org/lasers/pictures.cfm [Accessed March 31,2018]

[6] "Space Solar Power Institute", *William Cyrus Brown*, n.d., [Online]. Available:https://solarsat.org/billbrown_memorial.htm [Accessed March 31,2018]

[7] N. Shinohara, "Beam Efficiency of Wireless Power Transmission via Radio Waves from Short Range to Long Range", *Journal of the Korean Institute of Electromagnetic Engineering and Science*, Vol. 10, No. 4, December 2010

[8] D. Parker, D. C. Zimmermann, "Phased Arrays–Part II: Implementations, Applications, and Future Trends", *Microwave Theory and Techniques*, Vol. 50, No. 3, March 2002

[9] F. Akbar, A. Mortazawi, "Design of a Scalable Phased Array Antenna with a Simplified Architecture", *EuMC Microwave Conference*, University of Michigan, September 2015

[10] D. Ehyaie, "Novel Approaches to the Design of Phased Array Antennas", University of Michigan Doctor of Philosophy Dissertation, 2011

[11] R. J. Mailloux, Phased Array Antenna Handbook, Artech House, Inc., 1994, Norwood, MA.

[12] C. Balanis, Antenna Theory Analysis and Design, 3rd edition, J. Wiley and Sons, 2005

[13] X. Yang, W. Geyi, H. Sun, "Optimum Design of Wireless Power Transmission System Using Microstrip Patch Antenna Arrays," *IEEE Antennas Wireless Propagation Letters*, Vol. 16, 2017

[14] P. Zhu, Z. Ma, G. A. E. Vandenbosch, G. Gielen, "160 GHz Harmonic-Rejecting Antenna with CMOS Rectifier for Millimeter-Wave Wireless Power Transmission", *IEEE Antennas and Propagation*, 2015.

[15] "Wireless Power Transfer", "Resonant Inductive Coupling", *Wikipedia, the free encyclopedia*, n.d. [Online]. Available: https://en.wikipedia.org/wiki/Wireless_power_transfer [Accessed March 12, 2018]

[16] T. Horng, N. G. Alexopoulos, "Corporate Feed Design for Microstrip Arrays", *Antennas and Propagation*, Vol. 41, No. 12, December 1993

[17] "Tesla Coil", "Resonant Transformer", *Wikipedia, the free encyclopedia*, 2015 [Online]. Available: en.wikipedia.org/wiki/Tesla_coil, [Accessed March 12, 2018]

[18] E. Schaal, "A Glimpse at the Future of Electric Vehicle Charging", "Charging Pads", 2016 [Online]. Available:https://www.fleetcarma.com/electric-vehicle-charging-future/ [Accessed March 12, 2018]

[19] "Microstrip Mitred Bend Calculator", *Everything RF*, n.d. [Online]. Available: https://www.everythingrf.com/rf-calculators/microstrip-mitred-bend-calculator [Accessed March 31, 2018]

[20] "Animation Showing How a Phased Array Works", *Wikipedia, The Free Encyclopedia*, n.d. [Online]. Available: https://en.wikipedia.org/wiki/Phasedarray [Accessed April 19, 2018]

[21] "MP Antenna", "Hemispheric Antennas", [Online]. Available: http://www.mpantenna.com/omnidirectional-antenna-radiation-patterns [Accessed April 20, 2018]

[22] "Antenna Arrays And Python - Calculating Directivity", "Python Pandemonium", [Online]. Available: https://medium.com/python-pandemonium/antenna-arrays-and-python-calculating-directivity-84a2cfea0739 [Accessed April 20, 2018]

[23] B. Avser, J. Pierro, G. Rebeiz, Random Feeding Networks for Reducing the Number of Phase Shifters in Limited-Scan Arrays, IEEE Transactions on Antennas and Propagation, Vol. 64, No. 11, November 2016

[24] D. Ehyaie, A. Mortazawi, "A Modular Extended Resonance Transmit Array with Improved Scan Angle", *Microwave Symposium Digest*, 2009

[25] S. Vaccaro, D. L. del Rio, M. C. Vigano, "Phased arrays with reduced number of phase shifter bits for polarization and pointing control", *Antennas and Propagation Society International Symposium*, 2013

[26] M. J. Chik, W. Li, K. M. Cheng, "A 5 GHz, Integrated Transformer based, Variable Power Divider Design in CMOS Process", *2013 Asia-Pacific Microwave Conference Proceedings*, 2013

[27] A. Alkhateeb, N.Y. Nam, J. Zhang, R.W. Heath, "Massive MISO Combining with Switches", *IEEE Wireless Communication Letters*, Vol. 5, No. 3, June 2016

[28] C. Wolff, "Phase-increment Calculating", *Radar Basics*, n.d. [Online]. Available: http://www.radartutorial.eu/06.antennas/!an02.en.html [Accessed March 31,2018].

[29] S. Bulja, A. Grebennikov, "A novel power divider with continuous power division", *Microwave and Optical Technology Letters*, 55(7):1684-1686, July 2013

[30] "Mitered Bends", *Microwaves101.com*, n.d. [Online]. Available: https://www.microwaves101.com/encyclopedias/mitered-bends [Accessed March 31, 2018].

[31] S. Oh, J. Koo, M. Hwang, C. Park, Y. Jeong, J. Lim, K. Choi, D. Ahn, "An Unequal Wilkinson Power Divider with Variable Dividing Ratio", n.d. [Online]. Available: http://ieeexplore-ieee-org.proxy.ulib.uits.iu.edu/stamp/stamp.jsp?tp=&arnumber=4263836 [Accessed March 31, 2018].

[32] "DroneDefender C-UAS Device", *Battelle*, n.d. [Online]. Available: https://www.battelle.org/government-offerings/national-security/aerospace-systems/counter-UAS-technologies/dronedefender [Accessed March 31, 2018].

[33] "Why Just Detect Drones If You Can't Stop Them", *Drone Defense System*, 2018, [Online]. Available: http://www.dronedefense.systems [Accessed March 31, 2018]

[34] R. V. Gatti, A. Ocera, S. Bastioli, L. Marcaccioli, R. Sorrentino, "A Novel Compact Dual Band Reconfigurable Power Divider for Smart Antenna Systems", n.d. [Online]. Available: http://ieeexplore-ieee-org.proxy.ulib.uits.iu.edu/stamp/stamp.jsp?tp=&arnumber=4263839 [Accessed March 31, 2018].

[35] P. W. Hannan, "The Element-Gain Paradox for a Phased-Array Antenna", 1964. [Online]. Available: http://ieeexplore-ieee-org.proxy.ulib.uits.iu.edu/stamp/stamp.jsp?tp=&arnumber=1138237 [Accessed March 31, 2018]

[36] V. Rabinovich, N. Alexandrov, "Typical Array Geometries and Basic Beam Steering Methods," from *Antenna Arrays and Automotive Applications*, New York, NY: Springer New York, 2013.

[37] O. M. Bakr, M. Johnson, "Impact of phase and amplitude errors on arary performance", Electrical Engineering and Computer Sciences, UC Berkeley, January, 2009. [Online]. Available: https://www2.eecs.berkeley.edu/Pubs/TechRpts/2009/EECS-2009-1.pdf. Accessed: April 20, 2018

[38] J. C. Mankins, "A Fresh Look At Space Solar Power", Advanced Concepts Office, NASA Office of Space Access and Technology, Washington, DC. 20546. 1996.

[39] J. O. McSpadden, J. C. Mankins, "Space Solar Power Programs and Microwave Wireless Power Transmission Technology", *IEEE Microwave Magazine*, December 2002. [Online]. Available: http://ieeexplore-ieee-org.proxy.ulib.uits.iu.edu/stamp/stamp.jsp?tp=&arnumber=1145675 [Accessed March 31, 2018]

[40] A. Harris, "Beam It Down", *Engineering and Technology*, May 2013. [Online]. Available: http://ieeexplore-ieee-org.proxy.ulib.uits.iu.edu/stamp/stamp.jsp?tp=&arnumber=6513374 [Accessed March 31, 2018]

[41] P. Jaffe, "Sandwich Module Testing for Space Solar Power", *Aerospace Conference, IEEE*, 2013.

[42] P. Jaffe, J. Hodkin, F. Harrington, "Development of a Sandwich Module Prototype for Space Solar Power", *Aerospace Conference, IEEE*, 2012

[43] K. Li, K. See, W. Koh, J. Zhang, "Design of a 2.45 GHz Microwave Wireless Power Transfer System for Battery Charging Applications", *Nanyang Technological University, Singapore DSO National Laboratories*, 2017. [Online]. Available: http://ieeexplore-ieee-org.proxy.ulib.uits.iu.edu/stamp/stamp.jsp?tp=&arnumber=8293542 [Accessed March 31, 2018]

[44] R. Kashimura, T. Seki, K. Sakaguchi, "A Study of Rectenna Receiving Area Division for Microwave Wireless Power Transfer System", *Proceedings of 2017 Asia-Pacific Microwave Conference*, 2017

[45] J. Gavan, S. Tapuchi, "Microwave Wireless-Power Transmission to High-Altitude-Platform Systems", *The Radio Science Bulletin No 334*, September 2010

[46] Q. Chen, X. Chen, P. Feng, "A Comparative Study of Space Transmission Efficiency for the Microwave Wireless Transmission", *Proceedings of the 2015 Asia-Pacific Microwave Conference*, 2015

[47] M. R. Moorthi, A. Saravanakumar, "Rectenna Model for 2.45 GHz Microwave Wireless Power Transmission", *2013 International Conference on Energy Efficient Technologies for Sustainability*, 2013

[48] R. M. Dickinson, "Power in the Sky", *IEEE Microwave Magazine*, March 6, 2013. [Online]. Available: http://ieeexplore-ieee-org.proxy.ulib.uits.iu.edu/stamp/stamp.jsp?tp=&arnumber=6475357 [Accessed March 31, 2018]

[49] R. Tan, K. Jin, "A Novel Resonant-Linear Hybrid Converter Applied in microwave Wireless Power Transmission System", *2017 IEEE Applied Power Electronics Conference and Exposition (APEC)*, 2017

[50] M. Fairouz, M. Said, "Wireless Power Transfer Using Arrays with Automatic Beam Steering", *2016 Progress in Electromagnetic Research Symposium (PIERS)*, Shanghai, China, 8-11 August, 2016

[51] "AutoStore Robotic Shuttle System", *Puma Case Study*, n.d. [Online]. Available: https://goo.gl/images/RMMHsJ [Accessed Mar 31, 2018]

[52] W. L. Stutzman, G. A. Thiele, Antenna Theory and Design, 3rd Edition. New York: Wiley, 2013, p. 307

[53] S. Bulja, A. Grebennikov, "PIN Diode-Based Variable Directional Coupler", *Microwave and Optical Technology Letters*, Vol. 54, No. 11, November 2012

[54] T. Natarajan, "Basic Structure of microstrip patch antenna", *ResearchGate*, n.d. [Online]. Available: https://www.researchgate.net/publication/317823547_Slotted_and_Miniaturized_Patch_Antenna_for_WLAN_and_WiMAX_Applications/figures?lo=1 [Accessed April 23, 2018]

APPENDIX

A. APPENDIX–DESIGN NOTES, ADDITIONAL PLOTS, AND TABLES

Design Notes on Phased Arrays

For the sake of considering aspects of array design, we will take a drone defense application in a desert setting, where incidental stray power is not a major concern, but maximizing gain (and therefore efficiency) is. The best choice for this is a rectangular array with spacing of about one wavelength, maximizing directivity with no concern about grating lobes. Taking the array to be 100 x 100 elements, its total dimension will be 100 times the wavelength. How should we choose operating frequency? Ignoring any band licensing issues for the time being, we know that the "far-field" conditions will be present at:

$$R > 2 * D^2/\lambda \tag{A.1}$$

Higher frequency allows far-field to take effect at shorter distances, as well as making the array smaller and more portable, but system cost also rises with frequency. For a military application, function should outweigh the cost, and we select an operating frequency such that far-field of a standard "subarray" takes effect quickly, around a distance of 10 meters. Choosing this "minimum distance" distance is necessary because array behavior at closer distances is affected by mutual coupling [7], and therefore only Far-Field is considered. If we choose this "standard" to be when the system separates into eight 25 x 25 element subarrays, then D becomes 25 times lambda, and to satisfy the equation,

$$\lambda < 10/1250 \tag{A.2}$$

Which corresponds to a frequency of 37.5 GHz, and gives the entire array, composed of 10,000 elements, a size of just 0.8 x 0.8 meters.

Directivity Plots

For space considerations, the plots of rectangular array directivity as a function of steering angles for element spacings .68, .70, .80, and .90 lambda were omitted from the main body of this thesis. They are included here (Figures A.1, A.2, A.3, and A.4) for reference and for those who are curious about the development of the interesting phenomena contained therein.

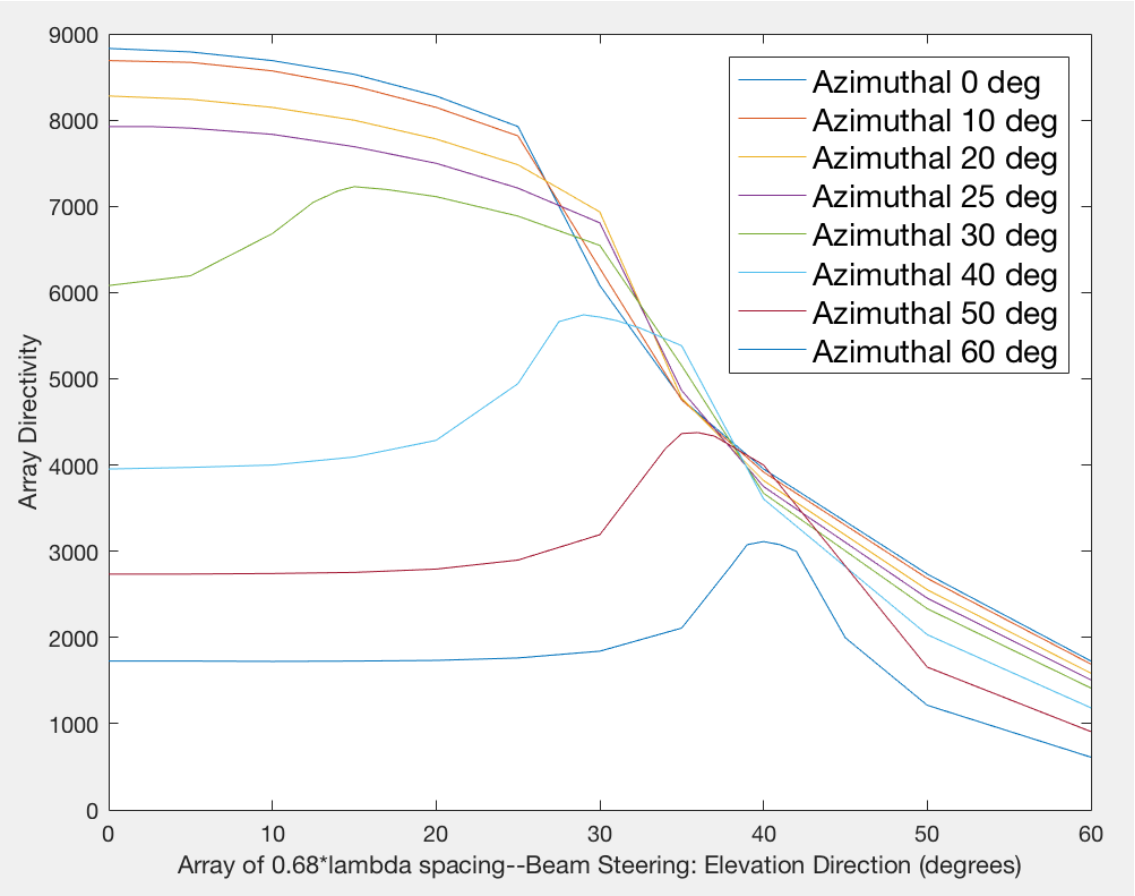

Fig. A.1. 39x39 Rectangular Array, 0.68 lambda spacing

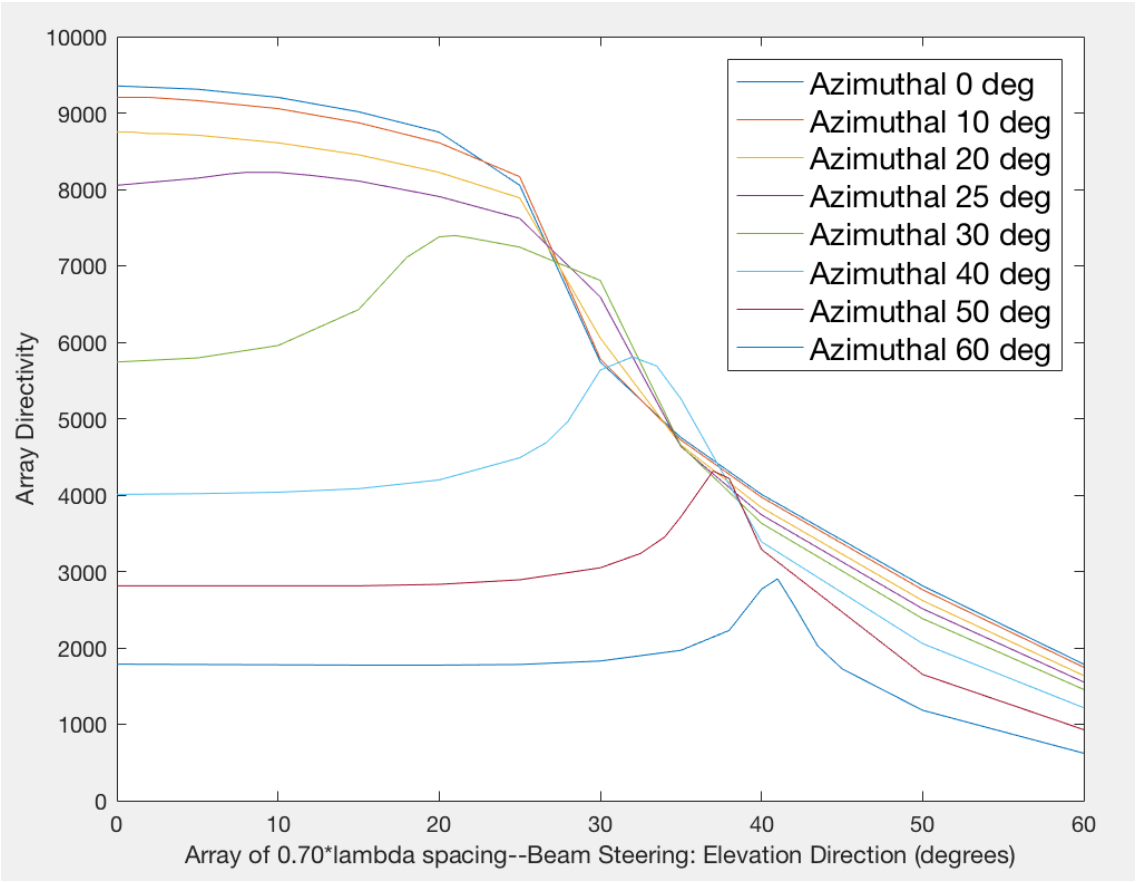

Fig. A.2. 39x39 Rectangular Array, 0.70 lambda spacing

Bill of Materials for Bypass Junction Test

In Figure A.5, the BOM is presented for the parts which were used to validate the bypass junction presented in Chapter 4.

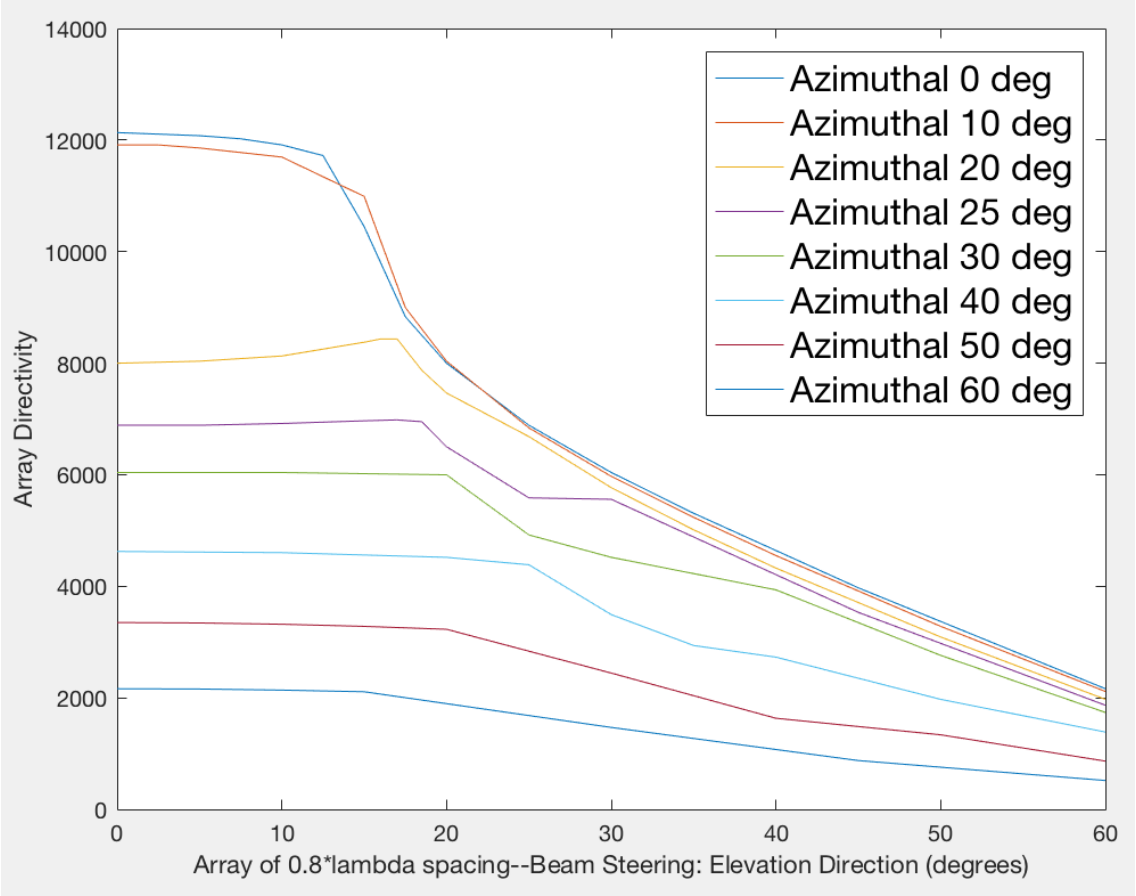

Fig. A.3. 39x39 Rectangular Array, 0.80 lambda spacing

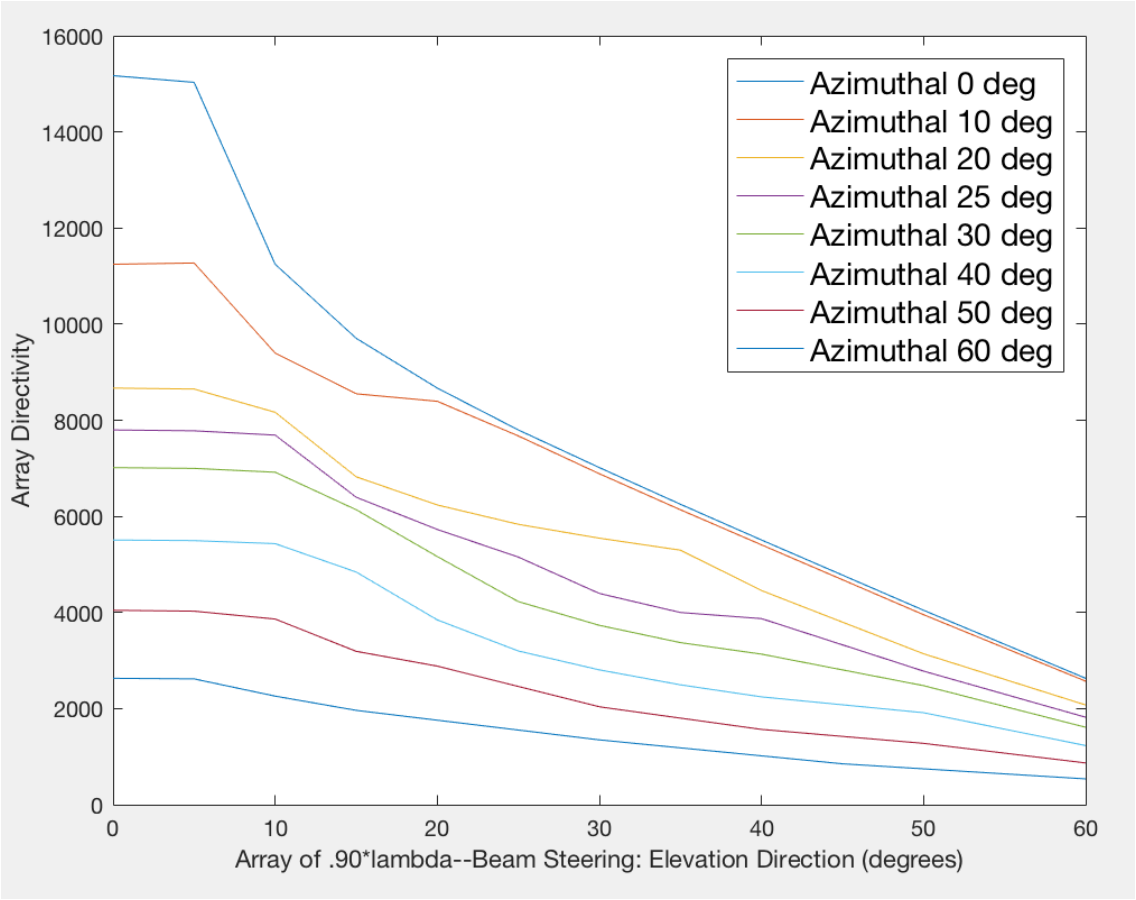

Fig. A.4. 39x39 Rectangular Array, 0.90 lambda spacing

BILL OF MATERIALS – BYPASS JUNCTION TEST

	Count	Manufacturer / Part
USB Signal Generator (operational at 2.4 GHz)	1	SG01 USB Signal Generator
Power Dividers / Combiners	3	Minicircuits ZX10-2-25-S+
RF Switches	2	Minicircuits ZFSWA-2-46
Spectrum Analyzer	1	Anritsu 8604A
DC Power Supply	2-4	LaVolta BPS305

Fig. A.5. BOM for Bypass Junction Test